Institute for Communications and Navigation

Baseline constrained ambiguity resolution with multiple frequencies

Patryk Jurkowski

A Thesis submitted for the Degree of
Bachelor of Science

Institute for Communications and Navigation

Prof. Dr. Christoph Günther

Supervised by Dr. Ing. Patrick Henkel

October 2010

Institute for Communications and Navigation

Technische Universität München
Theresienstrasse 90
80333 Munich

Acknowledgments

First, I would like to thank Prof. Dr. sc. nat. Christoph Günther for giving me the possibility of writing my Bachelor Thesis at his Institute. His great and selfless support of my interests even beyond this thesis was really impressive. He enabled me to have an insight into the wide range of scientific work.

I am greatly thankful to my supervisor, Dr. Patrick Henkel, who always gave me excellent and creative advises. His constant friendliness and helpful nature enabled a productive and pleasant working atmosphere. With his never fading enthusiasm for research and navigation he is also a great mentor for me.

My sincere thanks to Zhibo Wen, Sebastian Knogl and Kaspar Giger for their help and friendly discussions.

I am deeply grateful to my parents Mariola Jurkowski and Grzegorz Jurkowski for always supporting me with all their endeavour and advices, as well as my grandma Greta Musiałek for her interest in everything I do.

Especially, I would like to thank my girlfriend Birgit Wislsperger for brightening my life, day by day.

Contents

1 Introduction

Carrier phase measurements are extremely accurate but ambiguous. Integer ambiguity resolution is a common procedure in geodesy, e.g. for precise point positioning, for orbit estimation, for bias estimation, and for the positioning of reference stations. It is not yet done in safety-of-life critical applications due to the lack of sufficient reliability. In this thesis two techniques are discussed to substantially improve the reliability of carrier phase positioning.

First, the derivation of multi-frequency mixed code carrier linear combinations of Henkel and Günther [5] is reviewed. The use of both code and carrier phase measurements offers more degrees of freedom than a phase-only combination, i.e. it especially relaxes the integer constraints. The constraints on the combination design are a pre defined real-valued scaling of geometry and ionosphere suppression. The remaining degrees of freedom are used to minimize the combined noise level, maximizing the combined wavelength or maximizing the ambiguity discrimination. The latter one describes the ratio between combined noise level and combined wavelength, which is proportional to reliability of correct ambiguity estimation and the focus of this thesis.

Secondly, an a priori information about the baseline is taken into account in the ambiguity resolution. This information can be on the form of a length or direction constraint. It can be a tight constraint (i.e. a certain value) or a soft constraint allowing some variations. This thesis analyses both soft and tightly constraint ambiguity resolution and restricts to a priori information about the baseline length.

Both tightly and soft constrained ambiguity resolution have in common that the baseline estimate can no longer be separated with the ambiguity resolution by an orthogonal projection. The baseline a priori information occurs at two steps in the optimization: it is included in the constraint of the integer search tree, as well as in the baseline estimate for fixed ambiguities. This thesis provides the first method for soft constrained ambiguity resolution to our knowledge. It uses a cost function that achieves both the weighted range residuals and the difference between the length of the estimated baseline and the a priori assumed length. The minimization of the cost function includes an reliable search over ambiguity vectors, and an iterative computation of the baseline with the multivariate Newton algorithm. The confidence on the a priori knowledge is achieved in a weight of the a priori information. It is emphasized that this soft constrained ambiguity resolution, which is performed by a Lagrange optimization. The computation of the integer constraints also differs from the unconstrained case. At each node of the search tree, the consistency of the length of the baseline estimate with partial fixing and of the a priori knowledge is checked. Only those branches with a sufficient consistency are kept, which results in a dramatic improvement of both the search efficiency and the success rate. The constraint also allows a large search space volume, and, thereby, a further reduction of the error rate.

2 Multi-frequency code carrier linear combinations

The first option is to perform linear combinations over satellites, i.e. a satellite-satellite single difference measurement, which is used to remove the clock offset of the receiver and the phase and code bias of the receiver. The second option is to combine measurements from multiple receivers, e.g. on a receiver-receiver single difference, which removes the clock offset of a satellite and the phase and code bias of a satellite. Both options can be combined to the double difference measurements, that are the basis for RTK methods and orbit determination with a global network of reference stations (e.g. BERNESE software IGS [14]). The third option is to make a linear combination over multiple frequencies. This enables a scaling of the wavelength as well as a scaling of the dispersive ionospheric phase delay. The linear combination also affects the noise level the multipath of the biases. The forth option is to include both code and carrier phase measurements on the combination. The carrier phase is benefiting from a low noise level but it is ambiguous, while the code is unambiguous but more noisy. Thus, the code measurements relax the integer constraint of the combination. All four options are combined in this thesis, i.e. the multi-frequency linear combination of code and carrier phase measurements are computed from double difference measurements.

The basis of all types of linear combination are the code and carrier phase measurements as provided by the delay locked loop and phase locked loop. For the carrier phase, the following model is assumed:

$$\begin{aligned}\lambda_m \phi_{u,m}^k = r_u^k + \delta r_u^k + c\left(\delta\tau_u - \delta\tau^k\right) - q_{1m}^2 I_u'^k - \frac{1}{2} q_{1m}^3 I_u''^k + T_u^k + \lambda_m N_{u,m}^k \\ + b_{\phi_{u,m}} + b_{\phi_m^k} + \ddot{o}_{\phi_{u,m}^k} + \varepsilon_{\phi_{u,m}^k},\end{aligned} \tag{2.1}$$

with user u, satellite k, frequency m, wavelength λ_m, the carrier phase measurement $\phi_{u,m}^k$, range r_u^k between receiver u and satellite k, the projected orbital error δr_u^k, the receiver clock error $\delta\tau_u$, the satellite clock error $\delta\tau^k$, the ionospheric delays of first and second order $I_u'^k$ and $I_u''^k$ on L1, the ratio of frequencies $q_{1,m} = \frac{f_1}{f_m}$, the tropospheric delay T_u^k, the integer ambiguity $N_{u,m}^k$ between receiver u and satellite k, the receiver hardware phase bias $b_{\phi_{u,m}}$, the satellite hardware phase bias $b_{\phi_m^k}$, the superposed multipath phase error $\ddot{o}_{\phi_{u,m}^k}$ and carrier phase noise $\varepsilon_{\phi_{u,m}^k}$. A similar model is used for the code measurement

$$\begin{aligned}\rho_{u,m}^k = r_u^k + \delta r_u^k + c\left(\delta\tau_u - \delta\tau^k\right) + q_{1m}^2 I_u'^k + \frac{1}{2} q_{1m}^3 I_u''^k + T_u^k \\ + b_{\rho_{u,m}} + b_{\rho_m^k} + \ddot{o}_{\rho_{u,m}^k} + \varepsilon_{\rho_{u,m}^k}.\end{aligned} \tag{2.2}$$

Computing the linear combination with weight α_m for carrier phase measurement on frequency m and β_m for the code measurement gives:

$$\sum_{m=1}^{M} \left(\alpha_m \lambda_m \phi_{u,m}^k + \beta_m \rho_{u,m}^k \right) \tag{2.3}$$

$$= \left(r_u^k + \delta r_u^k + c \left(\delta\tau_u - \delta\tau^k \right) + T_u^k \right) \cdot \left(\sum_{m=1}^{M} \left(\alpha_m + \beta_m \right) \right) \tag{2.4}$$

$$+ I_{u,1}^{\prime k} \left(\sum_{m=1}^{M} \left(\alpha_m - \beta_m \right) q_{1m}^2 \right) \tag{2.5}$$

$$+ I_{u,1}^{\prime\prime k} \left(\sum_{m=1}^{M} \left(\frac{1}{2}\alpha_m - \beta_m \right) q_{1m}^3 \right) \tag{2.6}$$

$$+ \sum_{m=1}^{M} \left(\alpha_m \lambda_m N_m \right) \tag{2.7}$$

$$+ \sum_{m=1}^{M} \left(\alpha_m \left(b_{\phi_{u,m}} + b_{\phi_m^k} \right) + \beta_m \left(b_{\rho_{u,m}} + b_{\rho_m^k} \right) \right) \tag{2.8}$$

$$+ \sum_{m=1}^{M} \left(\alpha_m \ddot{o}_{\phi_{u,m}^k} + \beta_m \ddot{o}_{\rho_{u,m}^k} \right) \tag{2.9}$$

$$+ \sum_{m=1}^{M} \left(\alpha_m \varepsilon_{\phi_{u,m}^k} + \beta_m \varepsilon_{\rho_{u,m}^k} \right). \tag{2.10}$$

The choice of these weights α_m and β_m provides several degrees of freedom, which can be used to formulate constraints on the right sides of each term of (2.4) - (2.10).

The first term (2.4) describes the geometry which can be scaled to any arbitrary value

$$\sum_{m=1}^{M} \left(\alpha_m + \beta_m \right) = h_1, \quad h_1 \in \mathbb{R} \tag{2.11}$$

A geometry-free combination is obtained if $h_1 = 0$ and a geometry-preserving one if $h_1 = 1$. The value of h_1 also affects the orbital error and the receiver and satellite clock error as well as the tropospheric delay.

The second term (2.5) and third term (2.6) describe the influence of the ionospheric delay of first and second order on the combination dependent on the choice of the scaling factors α_m and β_m. This influence can be scaled by h_2 and h_3

$$\sum_{m=1}^{M} \left(\alpha_m - \beta_m \right) q_{1m}^2 = h_2, \quad h_2 \in \mathbb{R} \tag{2.12}$$

$$\sum_{m=1}^{M} \left(\frac{1}{2}\alpha_m + \beta_m \right) q_{1m}^3 = h_3, \quad h_3 \in \mathbb{R} \tag{2.13}$$

where $h_2 = 0$, $h_3 = 0$ corresponds to an ionosphere-free and $h_2 = 1$, $h_3 = 1$ to an ionosphere-preserving combination. Scaling this term with an arbitrary value in between 0 and 1 could be used to achieve a desired ionospheric suppression without various drawbacks due to a tight ionosphere-free constraint. Therefore, the value could be adapted to already achieved ionospheric suppression by double differencing.

The term (2.7) describes the linear combination of integer ambiguities. Since a combination of integer numbers must also be an integer number, we can write

$$\sum_{m=1}^{M} \alpha_m \lambda_m N_m = \lambda N \quad \text{with} \quad N \in \mathbb{Z}, \tag{2.14}$$

and the common wavelength λ. Solving for N leads to

$$N = \sum_{m=1}^{M} \underbrace{\frac{\alpha_m \lambda_m}{\lambda}}_{=j_m} N_m, \tag{2.15}$$

where j_m has to be integer to preserve the integer nature of N. Solving for α_m gives the phase weight as

$$\alpha_m = \frac{j_m \lambda}{\lambda_m}. \tag{2.16}$$

The next term (2.8) describes the combined error due to hardware biases. In designing the combination, the combined worst-case bias can be constrained to a certain value $b_{\max}$ based on upper bounds for the individual biases on each frequency, i.e.

$$\sum_{m=1}^{M} |\alpha_m| \left(\left| b_{\phi_{u,m}} \right| + \left| b_{\phi_m^k} \right| \right) + |\beta_m| \left(\left| b_{\rho_{u,m}} \right| + \left| b_{\rho_m^k} \right| \right) \leq b_{\max} \tag{2.17}$$

Similar to bias error the superposition on multipath delay (2.9) can be upper bounded by desired $\ddot{o}_{\max}$, i.e.

$$\sum_{m=1}^{M} |\alpha_m| \cdot \left| \ddot{o}_{\phi_{u,m}^k} \right| + |\beta_m| \cdot \left| \ddot{o}_{\rho_{u,m}^k} \right| \leq \ddot{o}_{\max}, \tag{2.18}$$

where the multipath delays on carrier phase measurement $\ddot{o}_{\phi_{u,m}^k}$ and code measurement $\ddot{o}_{\rho_{u,m}^k}$ are modeled as

$$\ddot{o}_{\phi_{u,m}^k} = \ddot{o}_{\phi,0} \cdot e^{-\frac{E}{\gamma}} \tag{2.19}$$

$$\ddot{o}_{\rho_{u,m}^k} = \ddot{o}_{\rho,0} \cdot e^{-\frac{E}{\gamma}}, \tag{2.20}$$

with the decay constant γ, the elevation angle E, and the delays $\ddot{o}_{\phi,0}$, $\ddot{o}_{\rho,0}$ for 0° elevation.

The last term (2.10) describes the combination of phase and code noise. It can be also included in design the combination, e.g. by minimizing the variance

$$\left(\sigma_u^k\right)^2 = \sum_{m=1}^{M} \left(\alpha_m^2 \sigma^2_{\varepsilon_{\phi^k_{u,m}}} + \beta_m^2 \sigma^2_{\varepsilon_{\rho^k_{u,m}}} \right). \tag{2.21}$$

Alternatively it is possible to maximize the ambiguity discrimination

$$D = \frac{\lambda}{2\sigma_u^k}, \tag{2.22}$$

which was first introduced by Henkel and Günther in [9]. This is especially useful if the focus lies on minimizing the probability of wrong fixing rather than on high accuracy.

To simplify notation we define an over-all phase sum:

$$w_\phi = \sum_{m=1}^{M} \alpha_m = \lambda \sum_{m=1}^{M} \frac{j_m}{\lambda_m} \tag{2.23}$$

and solving this definition for λ gives

$$\lambda = \frac{w_\phi}{\sum\limits_{m=1}^{M} \frac{j_m}{\lambda_m}}. \tag{2.24}$$

Setting this into (2.16) leads to

$$\alpha_m = \frac{j_m}{\lambda_m}\lambda = \frac{j_m}{\lambda_m} \frac{1}{\sum\limits_{m=1}^{M} \frac{j_m}{\lambda_m}} w_\phi. \tag{2.25}$$

We replace the phase weights in (2.11) and (2.12) by (2.25) and get a linear system of equations for the geometry and first order ionospheric combination which we write in matrix vector notation as

$$\mathbf{\Theta}_1 \begin{bmatrix} \beta_1 \\ \beta_2 \end{bmatrix} + \mathbf{\Theta}_2 \begin{bmatrix} w_\phi \\ \beta_3 \\ \vdots \\ \beta_M \end{bmatrix} = \begin{bmatrix} h_1 \\ h_2 \end{bmatrix}. \tag{2.26}$$

The ionospheric delay of second order in general is small enough for most safety critical applications, so that it is neglected in the further analysis. The two matrices $\mathbf{\Theta}_1$ and $\mathbf{\Theta}_2$ are only dependent on constants and are defined as

$$\mathbf{\Theta}_1 = \begin{bmatrix} 1 & 1 \\ -1 & -q_{12}^2 \end{bmatrix} \tag{2.27}$$

and

$$\boldsymbol{\Theta}_2 = \begin{bmatrix} 1 & 1 & \dots & 1 \\ \sum_{m=1}^{M} \frac{j_m}{\lambda_m} \frac{1}{\sum_{m=1}^{M} \frac{j_m}{\lambda_m}} q_{1m}^2 & -q_{13}^2 & \dots & q_{1M}^2 \end{bmatrix}. \tag{2.28}$$

Solving the linear system of equations (2.26) for β_1 and β_2 leads to

$$\begin{bmatrix} \beta_1 \\ \beta_2 \end{bmatrix} = \boldsymbol{\Theta}_1^{-1} \left(\begin{bmatrix} h_1 \\ h_2 \end{bmatrix} - \boldsymbol{\Theta}_2 \begin{bmatrix} w_\phi \\ \beta_3 \\ \vdots \\ \beta_M \end{bmatrix} \right) \tag{2.29}$$

$$= \begin{bmatrix} s_1 + s_2 w_\phi + \sum_{m=3}^{M} s_m \beta_m \\ t_1 + t_2 w_\phi + \sum_{m=3}^{M} t_m \beta_m \end{bmatrix} \tag{2.30}$$

where $s_i, t_i, i \in \{1, \dots, M\}$ are defined implicitly by equation (2.29). The ambiguity discrimination can be rewritten with (2.21), (2.22), (2.24), (2.25) and (2.30) as

$$\begin{aligned} D(w_\phi, \boldsymbol{\beta}) &= \frac{\lambda}{2\sigma} \\ &= \frac{w_\phi}{\sum_{m=1}^{M} \frac{j_m}{\lambda_m}} \cdot \frac{1}{2\sqrt{\tilde{\eta}^2 w_\phi^2 + \left(s_1 + s_2 w_\phi + \boldsymbol{s}^T \boldsymbol{\beta}\right)^2 \sigma_{\rho_1}^2 + \left(t_1 + t_2 w_\phi + \boldsymbol{t}^T \boldsymbol{\beta}\right)^2 \sigma_{\rho_2}^2 + \boldsymbol{\beta}^T \boldsymbol{\Sigma} \boldsymbol{\beta}}} \end{aligned} \tag{2.31}$$

with the definitions

$$\tilde{\eta}^2 = \sum_{m=1}^{M} \frac{j_m^2}{\lambda_m^2} \frac{1}{\left(\sum_{m=1}^{M} \frac{j_m}{\lambda_m} \right)^2} \sigma_{\phi_m}^2 \tag{2.32}$$

and

$$\boldsymbol{\Sigma} = \begin{bmatrix} \sigma_{\rho_3}^2 & \dots & \sigma_{\rho_3 \rho_M} \\ \vdots & \ddots & \vdots \\ \sigma_{\rho_3 \rho_M} & \dots & \sigma_{\rho_M}^2 \end{bmatrix} \tag{2.33}$$

as well as

$$\boldsymbol{\beta} = \begin{bmatrix} \beta_3 \\ \beta_4 \\ \vdots \\ \beta_M \end{bmatrix}, \quad \boldsymbol{s} = \begin{bmatrix} s_3 \\ s_4 \\ \vdots \\ s_M \end{bmatrix} \quad \text{and} \quad \boldsymbol{t} = \begin{bmatrix} t_3 \\ t_4 \\ \vdots \\ t_M \end{bmatrix}. \tag{2.34}$$

Maximization of the ambiguity discrimination (2.31) with respect to $\boldsymbol{\beta}$ leads to

$$\begin{aligned}\frac{\partial D}{\partial \boldsymbol{\beta}} &= \left(s_1 + s_2 w_\phi + \boldsymbol{s}^T\boldsymbol{\beta}\right)\boldsymbol{s}\cdot\sigma_{\rho_1}^2 + \left(t_1 + t_2 w_\phi + \boldsymbol{t}^T\boldsymbol{\beta}\right)\boldsymbol{t}\cdot\sigma_{\rho_2}^2 + \boldsymbol{\Sigma}\boldsymbol{\beta} \\ &= \sigma_{\rho_1}^2\boldsymbol{s}\left(s_1 + s_2 w_\phi + \boldsymbol{s}^T\boldsymbol{\beta}\right) + \sigma_{\rho_2}^2\boldsymbol{t}\left(t_1 + t_2 w_\phi + \boldsymbol{t}^T\boldsymbol{\beta}\right) + \boldsymbol{\Sigma}\boldsymbol{\beta} \\ &= \underbrace{\left(\sigma_{\rho_1}^2\boldsymbol{s}\boldsymbol{s}^T + \sigma_{\rho_2}^2\boldsymbol{t}\boldsymbol{t}^T + \boldsymbol{\Sigma}\right)}_{\boldsymbol{A}}\boldsymbol{\beta} + \underbrace{\left(s_2\sigma_{\rho_1}^2\boldsymbol{s} + t_2\sigma_{\rho_2}^2\boldsymbol{t}\right)}_{\boldsymbol{b}} w_\phi + \underbrace{\left(s_1\sigma_{\rho_1}^2\boldsymbol{s} + t_1\sigma_{\rho_2}^2\boldsymbol{t}\right)}_{\boldsymbol{c}} \stackrel{!}{=} \boldsymbol{0}\end{aligned} \tag{2.35}$$

and solving for $\boldsymbol{\beta}$ gives us the compact expression:

$$\boldsymbol{\beta} = -\boldsymbol{A}^{-1}\left(\boldsymbol{c} + \boldsymbol{b}\cdot w_\phi\right). \tag{2.36}$$

Analog to (2.35), we maximize the ambiguity discrimination (2.31) with respect to w_ϕ and get

$$\begin{aligned}\frac{\partial D}{\partial w_\phi} &= \left(s_1 + s_2 w_\phi + \boldsymbol{s}^T\boldsymbol{\beta}\right)\left(s_1 + \boldsymbol{s}^T\boldsymbol{\beta}\right)\sigma_{\rho_1}^2 \\ &\quad + \left(t_1 + t_2 w_\phi + \boldsymbol{t}^T\boldsymbol{\beta}\right)\left(t_1 + \boldsymbol{t}^T\boldsymbol{\beta}\right)\sigma_{\rho_2}^2 + \boldsymbol{\beta}^T\boldsymbol{\Sigma}\boldsymbol{\beta} \stackrel{!}{=} 0.\end{aligned} \tag{2.37}$$

Replacing $\boldsymbol{\beta}$ by (2.36) leads to

$$\begin{aligned}&\left(s_1 + s_2 w_\phi - \boldsymbol{s}^T\boldsymbol{A}^{-1}\left(\boldsymbol{c} + \boldsymbol{b}w_\phi\right)\right)\cdot\left(s_1 - \boldsymbol{s}^T\boldsymbol{A}^{-1}\left(\boldsymbol{c} + \boldsymbol{b}w_\phi\right)\right)\sigma_{\rho_1}^2 \\ &+ \left(t_1 + t_2 w_\phi - \boldsymbol{t}^T\boldsymbol{A}^{-1}\left(\boldsymbol{c} + \boldsymbol{b}w_\phi\right)\right)\cdot\left(t_1 - \boldsymbol{t}^T\boldsymbol{A}^{-1}\left(\boldsymbol{c} + \boldsymbol{b}w_\phi\right)\right)\sigma_{\rho_2}^2 \\ &+ \left(\boldsymbol{c} + \boldsymbol{b}w_\phi\right)^T\left(\boldsymbol{A}^{-1}\right)^T\boldsymbol{\Sigma}\boldsymbol{A}^{-1}\left(\boldsymbol{c} + \boldsymbol{b}w_\phi\right) = 0,\end{aligned} \tag{2.38}$$

which is a quadratic equation in w_ϕ, which can be rewritten as

$$r_0 + r_1\cdot w_\phi + r_2\cdot w_\phi^2 = 0 \tag{2.39}$$

with

$$r_0 = \left(s_1 - \boldsymbol{s}^T\boldsymbol{A}^{-1}\boldsymbol{c}\right)^2\sigma_{\rho_1}^2 + \left(t_1 - \boldsymbol{t}^T\boldsymbol{A}^{-1}\boldsymbol{c}\right)^2\sigma_{\rho_2}^2 + \boldsymbol{c}^T\left(\boldsymbol{A}^{-1}\right)^T\boldsymbol{\Sigma}\boldsymbol{A}^{-1}\boldsymbol{c} \tag{2.40}$$

$$\begin{aligned}r_1 = &\left(\left(s_1 - \boldsymbol{s}^T\boldsymbol{A}^{-1}\boldsymbol{c}\right)\left(-\boldsymbol{s}^T\boldsymbol{A}^{-1}\boldsymbol{b}\right) + \left(s_2 - \boldsymbol{s}^T\boldsymbol{A}^{-1}\boldsymbol{b}\right)\left(s_1 - \boldsymbol{s}^T\boldsymbol{A}^{-1}\boldsymbol{c}\right)\right)\cdot\sigma_{\rho_1}^2 \\ &+ \left(\left(t_1 - \boldsymbol{t}^T\boldsymbol{A}^{-1}\boldsymbol{c}\right)\left(-\boldsymbol{t}^T\boldsymbol{A}^{-1}\boldsymbol{b}\right) + \left(t_2 - \boldsymbol{t}^T\boldsymbol{A}^{-1}\boldsymbol{b}\right)\left(t_1 - \boldsymbol{t}^T\boldsymbol{A}^{-1}\boldsymbol{c}\right)\right)\cdot\sigma_{\rho_2}^2 \\ &+ \left(\boldsymbol{c}^T\left(\boldsymbol{A}^{-1}\right)^T\boldsymbol{\Sigma}\boldsymbol{A}^{-1}\boldsymbol{b} + \boldsymbol{b}^T\left(\boldsymbol{A}^{-1}\right)^T\boldsymbol{\Sigma}\boldsymbol{A}^{-1}\boldsymbol{c}\right)\end{aligned} \tag{2.41}$$

$$\begin{aligned}r_2 = &\left(s_2 - \boldsymbol{s}^T\boldsymbol{A}^{-1}\boldsymbol{b}\right)\left(-\boldsymbol{s}^T\boldsymbol{A}^{-1}\boldsymbol{b}\right)\cdot\sigma_{\rho_1}^2 + \left(t_2 - \boldsymbol{t}^T\boldsymbol{A}^{-1}\boldsymbol{b}\right)\left(-\boldsymbol{t}^T\boldsymbol{A}^{-1}\boldsymbol{b}\right)\cdot\sigma_{\rho_2}^2 \\ &+ \boldsymbol{b}^T\left(\boldsymbol{A}^{-1}\right)^T\boldsymbol{\Sigma}\boldsymbol{A}^{-1}\boldsymbol{b}.\end{aligned} \tag{2.42}$$

With replacing $\boldsymbol{A}, \boldsymbol{b}, \boldsymbol{s}$ and $\boldsymbol{t}$ by their definitions in (2.35), it can be shown that $r_2 = 0$ holds true in any case. From (2.39) the optimal phase weight can be rewritten as

$$w_{\phi_{\text{opt}}} = -\frac{r_0}{r_1}. \tag{2.43}$$

Finally, the phase weights α_m and code weights β_m we are interested in can be computed from (2.25), (2.36) and (2.30). Henkel and Günther have computed triple frequency GP-IF-NP mixed code-carrier combinations of maximum ambiguity discrimination in [9]. The derivation of the weighting coefficients is generalized to 4 frequencies in [7] and to M frequencies in [6].

Single and double differenced measurements

Satellite-satellite single differences of the carrier and code phases are given by

$$\nabla\lambda\phi_{u,m} = \lambda\phi^k_{u,m} - \lambda\phi^l_{u,m} \quad \text{and} \quad \nabla\rho_{u,m} = \lambda\rho^k_{u,m} - \lambda\rho^l_{u,m}, \tag{2.44}$$

which eliminate the receiver clock offset, phase and code biases. Thus, (2.1) and (2.2) can be rewritten as

$$\begin{aligned}\nabla\lambda\phi_{u,m} = {} & r^{k,l}_u + \delta r^{k,l}_u + c\delta\tau^{k,l} - q^2_{1m} I'^{k,l}_u - \frac{1}{2} q^3_{1m} I''^{k,l}_u + T^{k,l}_u + \lambda_m N^{k,l}_{u,m} \\ & + b_{\phi^{k,l}_m} + \ddot{\text{o}}_{\phi^{k,l}_{u,m}} + \varepsilon_{\phi^{k,l}_{u,m}}\end{aligned} \tag{2.45}$$

and

$$\begin{aligned}\nabla\rho_{u,m} = {} & r^{k,l}_u + \delta r^{k,l}_u + c\delta\tau^{k,l} + q^2_{1m} I'^{k,l}_u + q^3_{1m} I''^{k,l}_u + T^{k,l}_u \\ & + b_{\rho^{k,l}_m} + \ddot{\text{o}}_{\rho^{k,l}_{u,m}} + \varepsilon_{\rho^{k,l}_{u,m}}\end{aligned} \tag{2.46}$$

where $[\bullet]^{k,l} = [\bullet]^k - [\bullet]^l$.

A similar expression is obtained for receiver-receiver single differences:

$$\nabla\lambda\phi^k_m = \lambda\phi^k_{u,m} - \lambda\phi^k_{r,m} \quad \text{and} \quad \nabla\rho^k_m = \rho^k_{u,m} - \rho^k_{r,m}, \tag{2.47}$$

which eliminates the satellite clock offset, phase and code biases, and can be written as

$$\begin{aligned}\nabla\lambda\phi^k_m = {} & r^k_{u,r} + \delta r^k_{u,r} + c\delta\tau_{u,r} - q^2_{1m} I'^k_{u,r} - \frac{1}{2} q^3_{1m} I''^k_{u,r} + T^k_{u,r} + \lambda_m N^k_{u,r,m} \\ & + b_{\phi_{u,r,m}} + \ddot{\text{o}}_{\phi^k_{u,r,m}} + \varepsilon_{\phi^k_{u,r,m}},\end{aligned} \tag{2.48}$$

and

$$\begin{aligned}\nabla\rho^k_m = {} & r^k_{u,r} + \delta r^k_{u,r} + c\delta\tau_{u,r} + q^2_{1m} I'^k_{u,r} + \frac{1}{2} q^3_{1m} I''^k_{u,r} + T^k_{u,r} \\ & + b_{\rho_{u,r,m}} + \ddot{\text{o}}_{\rho^k_{u,r,m}} + \varepsilon_{\rho^k_{u,r,m}},\end{aligned} \tag{2.49}$$

where $[\bullet]_{u,r} = [\bullet]_u - [\bullet]_r$. If the baseline length is sufficiently small, $I'^k_{u,r}$, $I''^k_{u,r}$, $T^k_{u,r}$ are negligible and (2.50) as well as (2.51) can be simplified once more to

$$\nabla\lambda\phi^k_m = r^k_{u,r} + \delta r^k_{u,r} + c\delta\tau_{u,r} + \lambda_m N^k_{u,r,m} + b_{\phi_{u,r,m}} + \ddot{\text{o}}_{\phi^k_{u,r,m}} + \varepsilon_{\phi^k_{u,r,m}} \tag{2.50}$$

and

$$\nabla\rho_m^k = r_{u,r}^k + \delta r_{u,r}^k + c\delta\tau_{u,r} + b_{\rho_{u,r,m}} + \ddot{o}_{\rho_{u,r,m}^k} + \varepsilon_{\rho_{u,r,m}^k}, \tag{2.51}$$

where $\boldsymbol{\xi} = \boldsymbol{x}_u - \boldsymbol{x}_r$ denotes the baseline vector between both receivers.

The double differences of the carrier and code measurements follow as

$$\begin{aligned}\Delta\nabla\lambda\phi_m &= \left(\lambda\phi_{u,m}^k - \lambda\phi_{r,m}^k\right) - \left(\lambda\phi_{u,m}^l - \lambda\phi_{r,m}^l\right) \\ &= r_{u,r}^{k,l} + \delta r_{u,r}^{k,l} + \lambda_m N_{u,r,m}^{k,l} + \ddot{o}_{\phi_{u,r,m}^{k,l}} + \varepsilon_{\phi_{u,r,m}^{k,l}}\end{aligned} \tag{2.52}$$

and

$$\begin{aligned}\Delta\nabla\rho_m &= \left(\rho_{u,m}^k - \rho_{r,m}^k\right) - \left(\rho_{u,m}^l - \rho_{r,m}^l\right) \\ &= r_{u,r}^{k,l} + \delta r_{u,r}^{k,l} + \ddot{o}_{\phi_{u,r,m}^{k,l}} + \varepsilon_{\phi_{u,r,m}^{k,l}}.\end{aligned} \tag{2.53}$$

The ranges are expressed as a function of the user and satellite position, i.e.

$$\begin{aligned}r_{u,r}^{k,l} &= \left(r_u^k - r_r^k\right) - \left(r_u^l - r_r^l\right) \\ &= \left(\boldsymbol{e}_u^k\right)^T\left(\boldsymbol{x}_u - \boldsymbol{x}^k\right) - \left(\boldsymbol{e}_r^k\right)^T\left(\boldsymbol{x}_r - \boldsymbol{x}^k\right) - \left(\boldsymbol{e}_u^l\right)^T\left(\boldsymbol{x}_u - \boldsymbol{x}^l\right) + \left(\boldsymbol{e}_r^l\right)^T\left(\boldsymbol{x}_r - \boldsymbol{x}^l\right)\end{aligned} \tag{2.54}$$

where $\boldsymbol{e}_u^k$ is the estimated line-of-sight unit vector pointing from satellite k to user position u. For the short baselines, the following assumptions are made

$$\boldsymbol{e}_u^k \approx \boldsymbol{e}_r^k \quad \text{and} \quad \boldsymbol{e}_u^l \approx \boldsymbol{e}_r^l, \tag{2.55}$$

which enables us to simplify (2.54) to

$$\begin{aligned}r_{u,r}^{k,l} &= \left(\boldsymbol{e}_u^k\right)^T\left(\boldsymbol{x}_u - \boldsymbol{x}^k - \boldsymbol{x}_r + \boldsymbol{x}^k\right) - \left(\boldsymbol{e}_u^l\right)^T\left(\boldsymbol{x}_u - \boldsymbol{x}^k - \boldsymbol{x}_r + \boldsymbol{x}^k\right) \\ &= \left(\left(\boldsymbol{e}_u^k\right)^T - \left(\boldsymbol{e}_u^l\right)^T\right)\left(\boldsymbol{x}_u - \boldsymbol{x}_r\right).\end{aligned} \tag{2.56}$$

For long baselines the following corrections has to be computed and added to (2.56):

$$r_{u,r,\text{corr}}^{k,l} = \left(\left(\boldsymbol{e}_u^k\right)^T - \left(\boldsymbol{e}_r^k\right)^T\right)\left(\boldsymbol{x}_r - \boldsymbol{x}^k\right) - \left(\left(\boldsymbol{e}_u^l\right)^T - \left(\boldsymbol{e}_r^l\right)^T\right)\left(\boldsymbol{x}_r - \boldsymbol{x}^l\right) \tag{2.57}$$

All other terms of (2.52) and (2.53) are defined as

$$\delta r_{u,r}^{k,l} = \left(\delta r_u^k - \delta r_r^k\right) - \left(\delta r_u^l - \delta r_r^l\right), \tag{2.58}$$

$$\lambda_m N_{u,r,m}^{k,l} = \lambda\left(\left(N_{u,m}^k - N_{r,m}^k\right) - \left(N_{u,m}^l - N_{r,m}^l\right)\right) \tag{2.59}$$

$$\ddot{o}_{\phi_{u,r,m}^{k,l}} = \left(\ddot{o}_{\phi_{u,m}^k} - \ddot{o}_{\phi_{r,m}^k}\right) - \left(\ddot{o}_{\phi_{u,m}^l} - \ddot{o}_{\phi_{r,m}^l}\right), \tag{2.60}$$

$$\varepsilon_{\phi_{u,r,m}^{k,l}} = \left(\varepsilon_{\phi_{u,m}^k} - \varepsilon_{\phi_{r,m}^k}\right) - \left(\varepsilon_{\phi_{u,m}^l} - \varepsilon_{\phi_{r,m}^l}\right). \tag{2.61}$$

In the further analysis, the notation will be simplified by omitting the receiver and satellite indices unless it is essential for the fully understanding.

3 Integer least squares estimation

3.1 Estimation of baseline and ambiguities - Problem decomposition

The baseline $\boldsymbol{\xi}$ and ambiguities $\boldsymbol{N}$ are obtained by the integer least-squares estimation, i.e.

$$\min_{\boldsymbol{\xi},\boldsymbol{N}} \|\boldsymbol{\Psi} - \boldsymbol{H}\boldsymbol{\xi} - \boldsymbol{A}\boldsymbol{N}\|^2_{\boldsymbol{\Sigma}^{-1}} \,. \tag{3.1}$$

This minimization problem was decomposed by Teunissen in [20] into three terms using a partitioned system of normal equations [18]. The ambiguity resolution is in general performed in two steps and is also described in [1] and [2]: First, a so called float solution is computed by disregarding the integer nature of ambiguities. Secondly, the float ambiguities are fixed to integers. This two-step procedure enables an efficient solution without loss of optimality, which can be shown from an orthogonal projection on the space of $\boldsymbol{H}$, i.e. first we introduce the projector $\boldsymbol{P}_H$ and its orthogonal $\boldsymbol{P}^{\perp}_H$

$$\boldsymbol{P}_H = \boldsymbol{H}\left(\boldsymbol{H}^T\boldsymbol{\Sigma}^{-1}\boldsymbol{H}\right)^{-1}\boldsymbol{H}^T\boldsymbol{\Sigma}^{-1} \tag{3.2}$$

$$\boldsymbol{P}^{\perp}_H = \mathbf{1} - \boldsymbol{P}_H \tag{3.3}$$

with their fundamental properties:

$$\boldsymbol{P}_H \cdot \boldsymbol{H} = \boldsymbol{H}\underbrace{\left(\boldsymbol{H}^T\boldsymbol{\Sigma}^{-1}\boldsymbol{H}\right)^{-1}\boldsymbol{H}^T\boldsymbol{\Sigma}^{-1}\boldsymbol{H}}_{\mathbf{1}} = \boldsymbol{H} \tag{3.4}$$

$$\boldsymbol{P}^{\perp}_H \cdot \boldsymbol{H} = \left(\mathbf{1} - \boldsymbol{P}_H\right)\boldsymbol{H} = \boldsymbol{H} - \boldsymbol{P}_H\boldsymbol{H} = \boldsymbol{H} - \boldsymbol{H} = \mathbf{0} \tag{3.5}$$

As $\boldsymbol{P}_H + \boldsymbol{P}^{\perp}_H = \mathbf{1}$, one we can write:

$$\min_{\boldsymbol{\xi},\boldsymbol{N}} \|\boldsymbol{\Psi} - \boldsymbol{H}\boldsymbol{\xi} - \boldsymbol{A}\boldsymbol{N}\|^2_{\boldsymbol{\Sigma}^{-1}} = \min_{\boldsymbol{\xi},\boldsymbol{N}} \left\| \left(\boldsymbol{P}_H + \boldsymbol{P}^{\perp}_H\right)\left(\boldsymbol{\Psi} - \boldsymbol{H}\boldsymbol{\xi} - \boldsymbol{A}\boldsymbol{N}\right)\right\|^2_{\boldsymbol{\Sigma}^{-1}} = \tag{3.6}$$

$$= \min_{\boldsymbol{\xi},\boldsymbol{N}} \left\| \boldsymbol{P}_H\left(\boldsymbol{\Psi} - \boldsymbol{H}\boldsymbol{\xi} - \boldsymbol{A}\boldsymbol{N}\right) + \boldsymbol{P}^{\perp}_H\left(\boldsymbol{\Psi} - \boldsymbol{H}\boldsymbol{\xi} - \boldsymbol{A}\boldsymbol{N}\right)\right\|^2_{\boldsymbol{\Sigma}^{-1}} \tag{3.7}$$

$$= \min_{\boldsymbol{\xi},\boldsymbol{N}} \left\| \boldsymbol{P}_H\left(\boldsymbol{\Psi} - \boldsymbol{A}\boldsymbol{N}\right) - \underbrace{\boldsymbol{P}_H\boldsymbol{H}\boldsymbol{\xi}}_{=\boldsymbol{H}\boldsymbol{\xi}} + \boldsymbol{P}^{\perp}_H\left(\boldsymbol{\Psi} - \boldsymbol{A}\boldsymbol{N}\right) - \underbrace{\boldsymbol{P}^{\perp}_H\boldsymbol{H}\boldsymbol{\xi}}_{=\mathbf{0}} \right\|^2_{\boldsymbol{\Sigma}^{-1}} \tag{3.8}$$

The third term $\boldsymbol{P}_H^{\perp}(\Psi - \boldsymbol{A}\boldsymbol{N})$ is orthogonal with respect to the first two ones, so that the minimization over two variables is split into two minimizations over one variable:

$$\min_{\boldsymbol{\xi},\boldsymbol{N}} \left\| \boldsymbol{P}_H(\boldsymbol{\Psi} - \boldsymbol{A}\boldsymbol{N}) - \boldsymbol{H}\boldsymbol{\xi} + \boldsymbol{P}_H^{\perp}(\boldsymbol{\Psi} - \boldsymbol{A}\boldsymbol{N}) \right\|_{\boldsymbol{\Sigma}^{-1}}^2 = \tag{3.9}$$

$$= \min_{\boldsymbol{N}} \left(\left\| \boldsymbol{P}_H^{\perp}(\boldsymbol{\Psi} - \boldsymbol{A}\boldsymbol{N}) \right\|_{\boldsymbol{\Sigma}^{-1}}^2 + \min_{\boldsymbol{\xi}} \left\| \boldsymbol{P}_H(\boldsymbol{\Psi} - \boldsymbol{A}\boldsymbol{N}) - \boldsymbol{H}\boldsymbol{\xi} \right\|_{\boldsymbol{\Sigma}^{-1}}^2 \right) \tag{3.10}$$

These minimization will be further developed by introducing $\bar{\boldsymbol{A}} = \boldsymbol{P}_H^{\perp} \cdot \boldsymbol{A}$ and the projector $\boldsymbol{P}_{\bar{\boldsymbol{A}}}$ and its orthogonal $\boldsymbol{P}_{\bar{\boldsymbol{A}}}^{\perp}$ given by

$$\boldsymbol{P}_{\bar{\boldsymbol{A}}} = \bar{\boldsymbol{A}} \left(\bar{\boldsymbol{A}}^T \boldsymbol{\Sigma}^{-1} \bar{\boldsymbol{A}} \right)^{-1} \bar{\boldsymbol{A}}^T \boldsymbol{\Sigma}^{-1} \tag{3.11}$$

$$\boldsymbol{P}_{\bar{\boldsymbol{A}}}^{\perp} = \mathbf{1} - \boldsymbol{P}_{\bar{\boldsymbol{A}}} \tag{3.12}$$

so that (3.10) is rewritten with $\boldsymbol{P}_{\bar{\boldsymbol{A}}}\boldsymbol{A} = \bar{\boldsymbol{A}}$ as

$$\begin{aligned}
&\min_{\boldsymbol{N}} \left(\left\| \left(\boldsymbol{P}_{\bar{\boldsymbol{A}}} + \boldsymbol{P}_{\bar{\boldsymbol{A}}}^{\perp} \right) \left(\boldsymbol{P}_H^{\perp}\boldsymbol{\Psi} - \bar{\boldsymbol{A}}\boldsymbol{N} \right) \right\|_{\boldsymbol{\Sigma}^{-1}}^2 + \min_{\boldsymbol{\xi}} \left\| \boldsymbol{P}_H(\boldsymbol{\Psi} - \boldsymbol{A}\boldsymbol{N}) - \boldsymbol{H}\boldsymbol{\xi} \right\|_{\boldsymbol{\Sigma}^{-1}}^2 \right) \\
&= \min_{\boldsymbol{N}} \left(\left\| \boldsymbol{P}_{\bar{\boldsymbol{A}}}\boldsymbol{P}_H^{\perp}\boldsymbol{\Psi} - \boldsymbol{P}_{\bar{\boldsymbol{A}}}\bar{\boldsymbol{A}}\boldsymbol{N} \right\|_{\boldsymbol{\Sigma}^{-1}}^2 + \left\| \boldsymbol{P}_{\bar{\boldsymbol{A}}}^{\perp}\boldsymbol{P}_H^{\perp}\boldsymbol{\Psi} - \boldsymbol{P}_{\bar{\boldsymbol{A}}}^{\perp}\bar{\boldsymbol{A}}\boldsymbol{N} \right\|_{\boldsymbol{\Sigma}^{-1}}^2 \right. \\
&\quad \left. + \min_{\boldsymbol{\xi}} \left\| \boldsymbol{P}_H(\boldsymbol{\Psi} - \boldsymbol{A}\boldsymbol{N}) - \boldsymbol{H}\boldsymbol{\xi} \right\|_{\boldsymbol{\Sigma}^{-1}}^2 \right) \\
&= \min_{\boldsymbol{N}} \left(\left\| \boldsymbol{P}_{\bar{\boldsymbol{A}}}\boldsymbol{\Psi} - \bar{\boldsymbol{A}}\boldsymbol{N} \right\|_{\boldsymbol{\Sigma}^{-1}}^2 + \left\| \boldsymbol{P}_{\bar{\boldsymbol{A}}}^{\perp}\boldsymbol{P}_H^{\perp}\boldsymbol{\Psi} \right\|_{\boldsymbol{\Sigma}^{-1}}^2 + \min_{\boldsymbol{\xi}} \left\| \boldsymbol{P}_H(\boldsymbol{\Psi} - \boldsymbol{A}\boldsymbol{N}) - \boldsymbol{H}\boldsymbol{\xi} \right\|_{\boldsymbol{\Sigma}^{-1}}^2 \right).
\end{aligned} \tag{3.13}$$

The second term $\left\| \boldsymbol{P}_{\bar{\boldsymbol{A}}}^{\perp}\boldsymbol{P}_H^{\perp}\boldsymbol{\Psi} \right\|_{\boldsymbol{\Sigma}^{-1}}^2$ describes the irreducible noise and, thus, is independent for the estimate of $\boldsymbol{N}$ and $\boldsymbol{\xi}$. Furthermore, Teunissen stated in [18] that this irreducible error can be written as a function of the float ambiguities and baseline estimate:

$$\left\| \boldsymbol{P}_{\bar{\boldsymbol{A}}}^{\perp}\boldsymbol{P}_H^{\perp}\boldsymbol{\Psi} \right\|_{\boldsymbol{\Sigma}^{-1}}^2 = \left\| \boldsymbol{\Psi} - \boldsymbol{H}\hat{\boldsymbol{\xi}} - \boldsymbol{A}\hat{\boldsymbol{N}} \right\|_{\boldsymbol{\Sigma}^{-1}}^2 \tag{3.14}$$

Moreover, the last term of (3.13) vanishes as there can always be found a $\boldsymbol{\xi}$ that perfectly fits to $\boldsymbol{P}_H(\boldsymbol{\Psi} - \boldsymbol{A}\boldsymbol{N})$. Thus, the integer estimation simplifies to

$$\min_{\boldsymbol{N}} \left\| \boldsymbol{P}_{\bar{\boldsymbol{A}}}\boldsymbol{\Psi} - \bar{\boldsymbol{A}}\boldsymbol{N} \right\|_{\boldsymbol{\Sigma}^{-1}}^2. \tag{3.15}$$

The float solution is given by

$$\hat{\boldsymbol{N}} = \left(\bar{\boldsymbol{A}}^T \boldsymbol{\Sigma}^{-1} \bar{\boldsymbol{A}} \right)^{-1} \bar{\boldsymbol{A}}^T \boldsymbol{\Sigma}^{-1} \boldsymbol{P}_H^{\perp}\boldsymbol{\Psi}. \tag{3.16}$$

Now, the first term in the last row of (3.13) is rewritten as a function of the float ambiguity $\hat{\boldsymbol{N}}$ instead of the raw measurement $\boldsymbol{\Psi}$:

$$\begin{aligned}
\left\|\boldsymbol{P}_{\bar{\boldsymbol{A}}}\boldsymbol{\Psi}-\bar{\boldsymbol{A}}\boldsymbol{N}\right\|_{\boldsymbol{\Sigma}^{-1}}^{2} &= \left\|\bar{\boldsymbol{A}}\hat{\boldsymbol{N}}-\bar{\boldsymbol{A}}\boldsymbol{N}\right\|_{\boldsymbol{\Sigma}^{-1}}^{2} \\
&= \left(\bar{\boldsymbol{A}}\hat{\boldsymbol{N}}-\bar{\boldsymbol{A}}\boldsymbol{N}\right)^{T}\boldsymbol{\Sigma}^{-1}\left(\bar{\boldsymbol{A}}\hat{\boldsymbol{N}}-\bar{\boldsymbol{A}}\boldsymbol{N}\right) \\
&= \left(\hat{\boldsymbol{N}}^{T}\bar{\boldsymbol{A}}^{T}-\boldsymbol{N}^{T}\bar{\boldsymbol{A}}^{T}\right)\boldsymbol{\Sigma}^{-1}\left(\bar{\boldsymbol{A}}\hat{\boldsymbol{N}}-\bar{\boldsymbol{A}}\boldsymbol{N}\right) \\
&= \left(\hat{\boldsymbol{N}}^{T}-\boldsymbol{N}^{T}\right)\bar{\boldsymbol{A}}^{T}\boldsymbol{\Sigma}^{-1}\bar{\boldsymbol{A}}\left(\hat{\boldsymbol{N}}-\boldsymbol{N}\right) \\
&= \left\|\hat{\boldsymbol{N}}-\boldsymbol{N}\right\|_{\boldsymbol{\Sigma}_{\hat{\boldsymbol{N}}}^{-1}}^{2}, \qquad (3.17)
\end{aligned}$$

where

$$\boldsymbol{\Sigma}_{\hat{\boldsymbol{N}}}=\left(\bar{\boldsymbol{A}}^{T}\boldsymbol{\Sigma}^{-1}\bar{\boldsymbol{A}}\right)^{-1}. \qquad (3.18)$$

The third part can be written in full terms as

$$\boldsymbol{P}_{H}\left(\boldsymbol{\Psi}-\boldsymbol{A}\boldsymbol{N}\right)-\boldsymbol{H}\boldsymbol{\xi}=\boldsymbol{H}\underbrace{\left(\boldsymbol{H}^{T}\boldsymbol{\Sigma}^{-1}\boldsymbol{H}\right)^{-1}\boldsymbol{H}^{T}\boldsymbol{\Sigma}^{-1}\left(\boldsymbol{\Psi}-\boldsymbol{A}\boldsymbol{N}\right)}_{\check{\boldsymbol{\xi}}(\boldsymbol{N})}-\boldsymbol{H}\boldsymbol{\xi}. \qquad (3.19)$$

Obviously, setting $\boldsymbol{\xi}=\hat{\boldsymbol{\xi}}$ makes this term to 0. Note that $\check{\boldsymbol{\xi}}\left(\boldsymbol{N}\right)$ is interpreted as Least squares solution of $\min_{\boldsymbol{\xi}}\left\|\boldsymbol{\Psi}-\boldsymbol{A}\boldsymbol{N}-\boldsymbol{H}\boldsymbol{\xi}\right\|_{\boldsymbol{\Sigma}^{-1}}^{2}$, i.e.

$$\check{\boldsymbol{\xi}}\left(\boldsymbol{N}\right)=\underset{\boldsymbol{\xi}}{\operatorname{argmin}}\left\|\boldsymbol{\Psi}-\boldsymbol{A}\boldsymbol{N}-\boldsymbol{H}\boldsymbol{\xi}\right\|_{\boldsymbol{\Sigma}^{-1}}^{2}=\left(\boldsymbol{H}^{T}\boldsymbol{\Sigma}^{-1}\boldsymbol{H}\right)^{-1}\boldsymbol{H}^{T}\boldsymbol{\Sigma}^{-1}\left(\boldsymbol{\Psi}-\boldsymbol{A}\boldsymbol{N}\right) \qquad (3.20)$$

In analogy to (3.17) we can write

$$\begin{aligned}
\min_{\boldsymbol{\xi}}\left\|\boldsymbol{P}_{H}\left(\boldsymbol{\Psi}-\boldsymbol{A}\boldsymbol{N}\right)-\boldsymbol{H}\boldsymbol{\xi}\right\|_{\boldsymbol{\Sigma}^{-1}}^{2} &= \min_{\boldsymbol{\xi}}\left\|\boldsymbol{H}\check{\boldsymbol{\xi}}\left(\boldsymbol{N}\right)-\boldsymbol{H}\boldsymbol{\xi}(\boldsymbol{N})\right\|_{\boldsymbol{\Sigma}^{-1}}^{2} \qquad (3.21) \\
&= \min_{\boldsymbol{\xi}}\left\|\check{\boldsymbol{\xi}}\left(\boldsymbol{N}\right)-\boldsymbol{\xi}(\boldsymbol{N})\right\|_{\boldsymbol{\Sigma}_{\check{\boldsymbol{\xi}}(\boldsymbol{N})}^{-1}}^{2} \qquad (3.22)
\end{aligned}$$

with

$$\boldsymbol{\Sigma}_{\check{\boldsymbol{\xi}}(\boldsymbol{N})}=\left(\boldsymbol{H}^{T}\boldsymbol{\Sigma}^{-1}\boldsymbol{H}\right)^{-1}. \qquad (3.23)$$

Using all simplifications we can write the minimization problem as

$$\min_{\boldsymbol{N}}\left(\left\|\hat{\boldsymbol{N}}-\boldsymbol{N}\right\|_{\boldsymbol{\Sigma}_{\hat{\boldsymbol{N}}}^{-1}}^{2}+\min_{\boldsymbol{\xi}}\left\|\check{\boldsymbol{\xi}}\left(\boldsymbol{N}\right)-\boldsymbol{\xi}(\boldsymbol{N})\right\|_{\boldsymbol{\Sigma}_{\check{\boldsymbol{\xi}}(\boldsymbol{N})}^{-1}}^{2}\right) \qquad (3.24)$$

For unconstrained ambiguity resolution, the second term disappears so that the ambiguity resolution and baseline estimation can be performed separately. It is important to notice that this is no longer possible with the introduction of baseline constraints. In this case, the second term can no longer be made to zero, and consequently, ambiguity resolution and baseline estimation have to be performed jointly.

3.2 Ambiguity fixing - The integer least square search tree and its sequential construction

The integer least-squares estimate is given by

$$\check{\boldsymbol{N}} = \underset{\boldsymbol{N}\in\mathbb{Z}^n}{\operatorname{argmin}} \left(\hat{\boldsymbol{N}} - \boldsymbol{N}\right)^T \boldsymbol{\Sigma}_{\hat{\boldsymbol{N}}}^{-1} \left(\hat{\boldsymbol{N}} - \boldsymbol{N}\right) \tag{3.25}$$

and efficiently computed by LAMBDA (Least-squares Ambiguity Decorrelation Adjustment) of Teunissen in [20] and [19]. The implementation aspects are described by de Jonge and Tiberius in [15]. The LAMBDA method is a well known approach to solve the integer least square problem. This method consists of two steps as also described in [1] and [2]. First a grid-preserving ambiguity transformation is applied on the estimated float ambiguities, i.e.

$$\hat{\boldsymbol{z}} = \boldsymbol{Z}\hat{\boldsymbol{N}} \tag{3.26}$$

To keep the integer nature of the ambiguities, $\boldsymbol{Z}$ and $\boldsymbol{Z}^{-1}$ must have integer entries and must be volume-preserving. The requirement of being volume-preserving is satisfied with

$$|\det \boldsymbol{Z}| = 1. \tag{3.27}$$

In the second step a search is performed on the transformed ambiguities $\hat{\boldsymbol{z}}$ referred to as S. Finally a back-transformation $\boldsymbol{Z}^{-1}$ has to be applied to get the fixed ambiguities in the original space. Thus, the whole LAMBDA method can be written in a compact way as

$$\check{\boldsymbol{N}} = \boldsymbol{Z}^{-1} S\left(\boldsymbol{Z}\hat{\boldsymbol{N}}\right). \tag{3.28}$$

In detail, the search is realized as follows. The transformed search space is given by

$$(\hat{\boldsymbol{z}} - \boldsymbol{z})^T \boldsymbol{\Sigma}_{\hat{\boldsymbol{z}}}^{-1} (\hat{\boldsymbol{z}} - \boldsymbol{z}) \leq \chi^2, \quad \boldsymbol{z} \in \mathbb{Z}^K \tag{3.29}$$

where χ^2 is a positive constant which defines the size of the search space and

$$\boldsymbol{\Sigma}_{\hat{\boldsymbol{z}}} = \boldsymbol{Z}\boldsymbol{\Sigma}_{\hat{\boldsymbol{N}}}\boldsymbol{Z}^T \tag{3.30}$$

is the covariance matrix of transformed ambiguity vector. The inverse covariance matrix is decomposed with the triangular decomposition into

$$\boldsymbol{\Sigma}_{\hat{\boldsymbol{z}}}^{-1} = \boldsymbol{L}^T\boldsymbol{D}\boldsymbol{L} \tag{3.31}$$

and (3.29) is rewritten as

$$\tilde{\boldsymbol{z}}^T\boldsymbol{L}^T\boldsymbol{D}\boldsymbol{L}\tilde{\boldsymbol{z}} \leq \chi^2 \quad \text{with} \quad \tilde{\boldsymbol{z}} = \hat{\boldsymbol{z}} - \boldsymbol{z}. \tag{3.32}$$

The decomposition leads to a lower triangular matrix

$$\boldsymbol{L} = \begin{bmatrix} 1 & 0 & 0 & \dots & 0 \\ L_{2,1} & 1 & 0 & \dots & 0 \\ L_{3,1} & L_{3,2} & 1 & \dots & 0 \\ \vdots & \vdots & \vdots & \ddots & \vdots \\ L_{K,1} & L_{K,2} & L_{K,3} & \dots & 1 \end{bmatrix}$$

and a diagonal matrix

$$\boldsymbol{D} = \begin{bmatrix} D_{1,1} & 0 & 0 & \dots & 0 \\ 0 & D_{2,2} & 0 & \dots & 0 \\ 0 & 0 & D_{3,3} & \dots & 0 \\ \vdots & \vdots & \vdots & \ddots & \vdots \\ 0 & 0 & 0 & \dots & D_{K,K} \end{bmatrix}.$$

Thus, inequality (3.32) can be written component wise as

$$\begin{aligned} & D_{1,1}\tilde{z}_1^2 + D_{2,2}\left(\tilde{z}_1 L_{2,1} + \tilde{z}_2\right)^2 + D_{3,3}\left(\tilde{z}_1 L_{3,1} + \tilde{z}_2 L_{3,2} + \tilde{z}_3\right)^2 + \dots \\ & + D_{K,K}\left(\sum_{j=1}^{K-1} L_{j,K}\tilde{z}_j + \tilde{z}_K\right)^2 \leq \chi^2 \end{aligned} \tag{3.33}$$

$$\sum_{i=1}^{K} D_{i,i}\left(\tilde{z}_i + \sum_{j=1}^{i-1} L_{j,i}\tilde{z}_j\right)^2 \leq \chi^2 \tag{3.34}$$

where $D_{i,i}^{-1} = \sigma^2_{\hat{z}_{i|1,\dots,i-1}}$ can be interpreted as conditional variance. Blewitt suggested a sequential ambiguity fixing called bootstrapping in [13], where the difference between float and fixed ambiguities is used to correct for the error done by this fixing. In accordance with Teunissen [11] the conditional ambiguities can be written as

$$\hat{z}_{i|1,\cdots,K-1} = \hat{z}_i - \sum_{j=1}^{i-1} \sigma_{\hat{z}_i \hat{z}_{j|1,\cdots,j-1}} \sigma^{-2}_{\hat{z}_{j|1,\cdots,j-1}} \left(\hat{z}_{j|1,\cdots,j-1} - \left[\hat{z}_{j|1,\cdots,j-1}\right]\right), \tag{3.35}$$

where $[\bullet]$ denotes the rounding, $\sigma_{\hat{z}_i \hat{z}_{j|1,\cdots,j-1}}$ describes the covariance between the unconditional and conditional float ambiguities and $\sigma^{-2}_{\hat{z}_{j|1,\cdots,j-1}}$ describes the conditional variance. Writing (3.34) in full terms gives

$$\sum_{i=1}^{K} \frac{\left(\left(\hat{z}_i - z_i\right) + \sum_{j=1}^{i-1} L_{j,i}\left(\hat{z}_j - z_j\right)\right)^2}{\sigma^2_{\hat{z}_{i|1,\dots,i-1}}} \leq \chi^2 \tag{3.36}$$

and equating the coefficients with (3.35) we can write (3.36) as sequential conditional adjustment

$$\sum_{i=1}^{K} \frac{\left(z_i - \hat{z}_{i|1,\ldots,i-1}\right)^2}{\sigma^2_{\hat{z}_{i|1,\ldots,i-1}}} \leq \chi^2, \tag{3.37}$$

with interpretation of $L_{j,i} = \sigma_{\hat{z}_i \hat{z}_{j|1,\cdots,j-1}} \sigma^{-2}_{\hat{z}_{j|1,\cdots,j-1}}$. The inequality (3.37) can be rearranged to

$$\begin{aligned} \frac{\left(z_i - \hat{z}_{i|1,\ldots,i-1}\right)}{\sigma^2_{\hat{z}_{i|1,\ldots,i-1}}} &\leq \chi^2 - \sum_{l=1}^{i-1} \frac{\left(z_l - \hat{z}_{l|1,\ldots,l-1}\right)^2}{\sigma^2_{\hat{z}_{l|1,\ldots,l-1}}} - \sum_{l=i+1}^{K} \frac{\left(z_l - \hat{z}_{l|1,\ldots,l-1}\right)^2}{\sigma^2_{\hat{z}_{l|1,\ldots,l-1}}} \\ &\leq \chi^2 - \sum_{l=1}^{i-1} \frac{\left(z_l - \hat{z}_{l|1,\ldots,l-1}\right)^2}{\sigma^2_{\hat{z}_{l|1,\ldots,l-1}}} \end{aligned} \tag{3.38}$$

and solving for the candidates z_i gives

$$\left|z_i - \hat{z}_{i|1,\ldots,i-1}\right| \leq \sigma_{\hat{z}_{i|1,\ldots,i-1}} \sqrt{\chi^2 - \sum_{l=1}^{i-1} \frac{\left(z_l - \hat{z}_{l|1,\ldots,l-1}\right)^2}{\sigma^2_{\hat{z}_{l|1,\ldots,l-1}}}}. \tag{3.39}$$

In common χ is determined by rounding the decorrelated ambiguities $\hat{\boldsymbol{z}} = \boldsymbol{Z}\hat{\boldsymbol{N}}$ to their closest integers and with $\check{\boldsymbol{N}}' = \boldsymbol{Z}^{-1}[\hat{\boldsymbol{z}}]$ we get

$$\chi^2 = \left(\hat{\boldsymbol{N}} - \check{\boldsymbol{N}}'\right)^T \boldsymbol{\Sigma}^{-1}_{\hat{\boldsymbol{N}}} \left(\hat{\boldsymbol{N}} - \check{\boldsymbol{N}}'\right). \tag{3.40}$$

With this brief view on the LAMBDA method it is obvious that a priori information about the baseline is not used in the search. In case of available constraints on the baseline as a priori information about the baseline length one has to compute a set of integer ambiguity vectors without using the available knowledge about the baseline and then apply a constrained ambiguity resolution method as described in chapter 5 on all of these candidates of ambiguity vectors delivered by LAMBDA. This is a draw back in computation performance of the search. During the bootstrap algorithm of LAMBDA where the float ambiguities are fixed one by one, integer vectors are computed, which are known to violate the baseline constraints. Buist suggested a method to limit the search space of LAMBDA in [10]. The C-LAMBDA method was introduced by [12] and [21], which integrates a constraint on baseline length into standard LAMBDA to reduce the time to first fix. To raise the computational performance of the baseline constrained ambiguity resolution we now introduce a method that integrates the a priori information about the baseline length into the search part of LAMBDA.

4 Constrained integer search

We start with the well known fixing of the first decorrelated ambiguity with (3.39)

$$|\check{z}_1 - \hat{z}_1| \leq \sigma_{\hat{z}_1}\sqrt{\chi^2} \quad \text{with} \quad \check{z}_1 \in \mathbb{Z} \tag{4.1}$$

which gives us a set of candidates for the first ambiguity. For each of these $\check{z}_1$ in the denoted interval we compute the common least square solution for the baseline and ambiguity vector which is designated as the mixed float fixed minimization problem

$$\min_{\boldsymbol{\xi},\boldsymbol{z}} \left\| \boldsymbol{\Psi} - \boldsymbol{H}\boldsymbol{\xi} - \boldsymbol{A}\left(\boldsymbol{Z}^T\right)^{-1}\boldsymbol{z} \right\|^2_{\boldsymbol{\Sigma}^{-1}}, \tag{4.2}$$

where

$$\boldsymbol{z} = \boldsymbol{P}_1\check{\boldsymbol{z}}_1 + \boldsymbol{P}_2\boldsymbol{z}_2 \tag{4.3}$$

denotes the separation of the mixed float fixed ambiguity vector into a fixed ambiguity vector $\check{\boldsymbol{z}}_1$ and a float ambiguity vector $\boldsymbol{z}_2$. After fixing the first decorrelated ambiguity with (4.1) the selection matrices $\boldsymbol{P}_1$ and $\boldsymbol{P}_2$ can be written as

$$\boldsymbol{P}_1 = \begin{bmatrix} 1 \\ 0 \\ \vdots \\ 0 \end{bmatrix}, \qquad \boldsymbol{z}_1 = \left[\check{z}_1\right], \qquad \boldsymbol{P}_2 = \begin{bmatrix} 0 & 0 & \dots & 0 \\ 1 & 0 & \dots & 0 \\ 0 & 1 & \dots & 0 \\ \vdots & \vdots & \ddots & \vdots \\ 0 & 0 & \dots & 1 \end{bmatrix}, \qquad \boldsymbol{z}_2 = \begin{bmatrix} z_2 \\ z_3 \\ \vdots \\ z_K \end{bmatrix}, \tag{4.4}$$

where $\boldsymbol{z}_1$ is one of fixed ambiguities from interval (4.1). $\boldsymbol{z}_2$ is the float ambiguity vector and has to be estimated. Then, the minimization problem (4.2) can be written as:

$$\min_{\boldsymbol{\xi},\boldsymbol{z}_2} \left\| \left(\boldsymbol{\Psi} - \boldsymbol{A}\left(\boldsymbol{Z}^T\right)^{-1}\boldsymbol{P}_1\check{\boldsymbol{z}}_1 \right) - \boldsymbol{H}\boldsymbol{\xi} - \boldsymbol{A}\left(\boldsymbol{Z}^T\right)^{-1}\boldsymbol{P}_2\boldsymbol{z}_2 \right\|^2_{\boldsymbol{\Sigma}^{-1}} \tag{4.5}$$

Computing the least-squares solution of $\hat{\boldsymbol{\xi}}(\check{\boldsymbol{z}}_1)$ with (4.5) for each of the candidates from (4.1) leads to a set of baseline estimates $\hat{\boldsymbol{\xi}}(\check{\boldsymbol{z}}_1)$. Now we will check each baseline candidate for satisfying the baseline length constraint described with the inequality

$$\left| \left\| \hat{\boldsymbol{\xi}}(\check{\boldsymbol{z}}_1) \right\| - l \right| \leq \mu\sigma_{\|\hat{\boldsymbol{\xi}}(\check{\boldsymbol{z}}_1)\|}. \tag{4.6}$$

l describes the a priori knowledge about the baseline length, μ is the confidence factor which describes the trust in the a priori information l. $\sigma_{\|\hat{\boldsymbol{\xi}}(\check{\boldsymbol{z}}_1)\|}$ denotes the standard deviation of the estimated baseline length defined as

$$\sigma_{\|\hat{\boldsymbol{\xi}}(\check{\boldsymbol{z}}_1)\|} = \sqrt{\sigma^2_{\hat{\boldsymbol{\xi}}_x} + \sigma^2_{\hat{\boldsymbol{\xi}}_y} + \sigma^2_{\hat{\boldsymbol{\xi}}_z}} = \sqrt{\operatorname{trace}\left(\boldsymbol{\Sigma}_{\hat{\boldsymbol{\xi}}(\check{\boldsymbol{z}}_1)}\right)}. \tag{4.7}$$

Now, only these candidates of inequality (4.1) are used whose baseline estimate (4.5) fulfills the constraint inequality (4.6). All other candidates are dropped.

This reduced set of candidates is used to fix the second ambiguity in the same manner as in LAMBDA. The inequality

$$\left|\check{z}_2 - \hat{z}_{2|1}\right| \leq \sigma_{\hat{z}_{2|1}} \sqrt{\chi^2 - \frac{\left(\check{z}_1 - \hat{z}_1\right)^2}{\sigma^2_{\hat{z}_1}}} \quad \text{with} \quad \check{z}_1 \in \mathbb{Z} \tag{4.8}$$

is now dependent on the previous fixed ambiguities $\check{z}_1$ and gives us a set of candidates for $\check{z}_2$. With the separated minimization problem (4.5) and the definitions

$$\boldsymbol{P}_1 = \begin{bmatrix} 1 & 0 \\ 0 & 1 \\ 0 & 0 \\ \vdots & \vdots \\ 0 & 0 \end{bmatrix}, \qquad \boldsymbol{z}_1 = \begin{bmatrix} \check{z}_1 \\ \check{z}_2 \end{bmatrix}, \qquad \boldsymbol{P}_2 = \begin{bmatrix} 0 & 0 & \dots & 0 \\ 0 & 0 & \dots & 0 \\ 1 & 0 & \dots & 0 \\ 0 & 1 & \dots & 0 \\ \vdots & \vdots & \ddots & \vdots \\ 0 & 0 & \dots & 1 \end{bmatrix}, \qquad \boldsymbol{z}_2 = \begin{bmatrix} z_3 \\ z_4 \\ \vdots \\ z_K \end{bmatrix} \tag{4.9}$$

for the selection matrices $\boldsymbol{P}_1$, $\boldsymbol{P}_2$, the fixed ambiguity vector $\boldsymbol{z}_1$ and float ambiguity vector $\boldsymbol{z}_2$, a further least-squares estimation of the mixed float fixed baseline $\hat{\boldsymbol{\xi}}(\check{\boldsymbol{z}}_1)$ and the float solution for $\boldsymbol{z}_2$ is computed. In analogy to the first ambiguity fixing the check on fulfilling the baseline constraint is performed with (4.6) on each $\hat{\boldsymbol{\xi}}(\check{\boldsymbol{z}}_1)$, which will again drop all candidates which do not fulfill the constraint on baseline length.

This procedure is continued for all remaining float ambiguities analogically. In general the method is to compute the candidates with inequality (3.39) and to evaluate the mixed float fixed solution for the baseline with equation (4.5) and

$$\boldsymbol{P}_1 = \begin{bmatrix} 1 & 0 & \dots & 0 \\ 0 & 1 & \dots & 0 \\ \vdots & \vdots & \ddots & \vdots \\ 0 & 0 & \dots & 1 \\ 0 & 0 & \dots & 0 \\ \vdots & \vdots & \ddots & \vdots \\ 0 & 0 & \dots & 0 \end{bmatrix} \in \mathbb{R}^{K \times (K-r)}, \qquad \boldsymbol{z}_1 = \begin{bmatrix} \check{z}_1 \\ \check{z}_2 \\ \vdots \\ \check{z}_{K-r} \end{bmatrix} \in \mathbb{R}^{(K-r)}, \tag{4.10}$$

$$\boldsymbol{P}_2 = \begin{bmatrix} 0 & 0 & \dots & 0 \\ \vdots & \vdots & \ddots & \vdots \\ 0 & 0 & \dots & 0 \\ 1 & 0 & \dots & 0 \\ 0 & 1 & \dots & 0 \\ \vdots & \vdots & \ddots & \vdots \\ 0 & 0 & \dots & 1 \end{bmatrix} \in \mathbb{R}^{K \times r}, \qquad \boldsymbol{z}_2 = \begin{bmatrix} z_{K-(r-1)} \\ z_{K-(r-2)} \\ \vdots \\ z_K \end{bmatrix} \in \mathbb{R}^{r}, \tag{4.11}$$

where r is the number of remaining unfixed ambiguities, for every candidate, as well as checking these baseline estimates to achieve the inequality (4.6).

This procedure is continued until the last set of ambiguities is fixed. Now we have a set of fixed and decorrelated ambiguity vectors which all fulfill the constraint on baseline length. If there is more than one ambiguity vector left, the cost function

$$J(\hat{\boldsymbol{\xi}}(\check{\boldsymbol{z}}_1), \check{\boldsymbol{z}}_1) = \mu' \left(\left\| \hat{\boldsymbol{\xi}}(\check{\boldsymbol{z}}_1) \right\| - l \right)^2 + \left\| \boldsymbol{\Psi} - \boldsymbol{H}\hat{\boldsymbol{\xi}}(\check{\boldsymbol{z}}_1) - \boldsymbol{A} \left(\boldsymbol{Z}^T \right)^{-1} \check{\boldsymbol{z}}_1 \right\|^2_{\boldsymbol{\Sigma}^{-1}} \tag{4.12}$$

is evaluated for each of them. Finally, the fixed ambiguity vector $\check{\boldsymbol{N}} = \left(\boldsymbol{Z}^T \right)^{-1} \check{\boldsymbol{z}}_1$ that minimizes the cost function is chosen as the estimated ambiguity vector. Note that the float solution is integer decorrelated before the integer search, to improve the success rate of sequential ambiguity fixing. A decorrelation at each node of the search tree has not been considered as this would substantially increase the complexity of the search.

Fig. (4.1) describes the method of integer ambiguity estimation in a graphical way. To simplify notation we rewrite inequality (3.39) which defines an interval for integer ambiguities to $l_{\hat{z}_i|1,\cdots,i-1} \leq \check{z}_i \leq u_{\hat{z}_i|1,\cdots,i-1}$ with with a lower bound

$$l_{\hat{z}_{i|1,\cdots,i-1}} = \hat{z}_{i|1,\ldots,i-1} - \sigma_{\hat{z}_{i|1,\ldots,i-1}} \sqrt{\chi^2 - \sum_{l=1}^{i-1} \frac{\left(z_l - \hat{z}_{l|1,\ldots,l-1} \right)^2}{\sigma^2_{\hat{z}_{l|1,\ldots,l-1}}}} \tag{4.13}$$

and an upper bound

$$u_{\hat{z}_{i|1,\cdots,i-1}} = \hat{z}_{i|1,\ldots,i-1} + \sigma_{\hat{z}_{i|1,\ldots,i-1}} \sqrt{\chi^2 - \sum_{l=1}^{i-1} \frac{\left(z_l - \hat{z}_{l|1,\ldots,l-1} \right)^2}{\sigma^2_{\hat{z}_{l|1,\ldots,l-1}}}}. \tag{4.14}$$

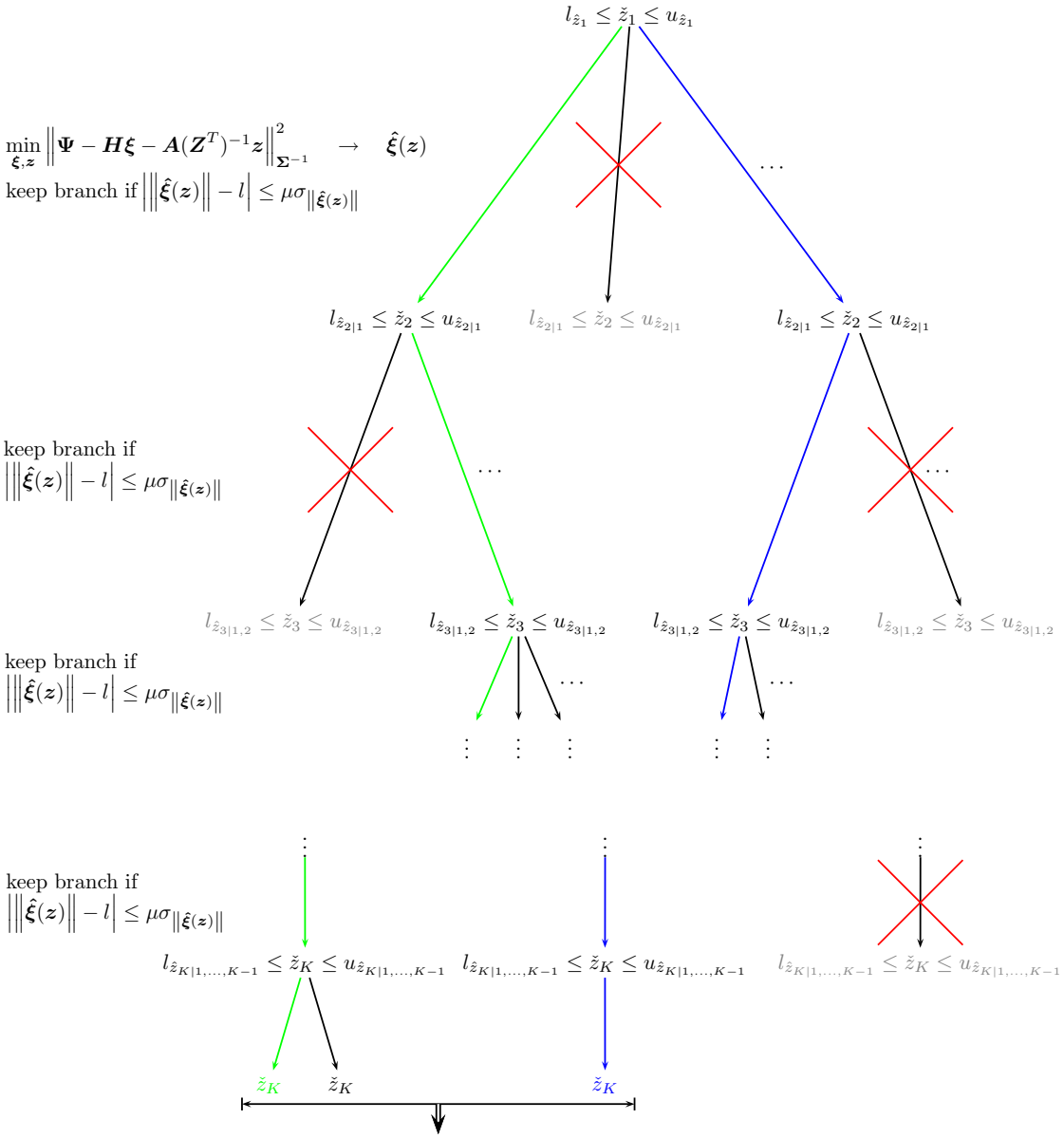

choose the final integer ambiguity vector from the remaining B ones, that fulfills

$$\min_{b=1\ldots B} \left(J(\hat{\boldsymbol{\xi}}(\check{\boldsymbol{z}}_{1,b}), \check{\boldsymbol{z}}_{1,b}) = \mu' \left(\left\| \hat{\boldsymbol{\xi}}(\check{\boldsymbol{z}}_{1,b}) \right\| - l \right)^2 + \left\| \boldsymbol{\Psi} - \boldsymbol{H}\hat{\boldsymbol{\xi}}(\check{\boldsymbol{z}}_{1,b}) - \boldsymbol{A}\left(\boldsymbol{Z}^T\right)^{-1} \check{\boldsymbol{z}}_{1,b} \right\|^2_{\boldsymbol{\Sigma}^{-1}} \right),$$

where $\check{\boldsymbol{z}}_{1,b}$ is fixed ambiguity vector candidate b (path) of all ambiguity vectors B that fulfill the baseline constraint e.g. $\hat{\boldsymbol{\xi}}(\check{\boldsymbol{z}}_{1,1}), \check{\boldsymbol{z}}_{1,1}$ and $\hat{\boldsymbol{\xi}}(\check{\boldsymbol{z}}_{1,3}), \check{\boldsymbol{z}}_{1,3}$.

Figure 4.1: Graphical representation of integrated, baseline constrained integer ambiguity resolution. Each full path through the tree is equivalent to a ambiguity vector. In this example there are $B = 3$ paths that fulfill the baseline length constraint.

5 Baseline constrained ambiguity resolution

Solving the minimization problem $\min_{\boldsymbol{\xi},\boldsymbol{N}} \|\boldsymbol{\Psi} - \boldsymbol{H}\boldsymbol{\xi} - \boldsymbol{A}\boldsymbol{N}\|^2_{\boldsymbol{\Sigma}^{-1}}$ over the two independent variables $\boldsymbol{\xi}$ and $\boldsymbol{N}$ yields to high computational effort usually. $\boldsymbol{\xi}$ is the baseline vector between the two receivers and has dimension 3. $\boldsymbol{N}$ describes the ambiguity vector and has the dimension of the number of visible satellites K in the case of not using differenced measurements and $K-1$ in case of double differences. A brute force search in a $K+2$ respectively $K+3$ dimensional space is impractical. However there are known methods for reducing the complexity. The LAMBDA method was introduced by Teunissen in [20] and [19] and has proven to be a efficient way to determine the integer ambiguity vector. LAMBDA was already briefly explained in the chapter 3 and was extended by the efficient determination of ambiguity vectors in the case of constraints on baseline length in chapter 4. A similar extension was suggested by [16], where additional constraints on yaw and pitch angle were introduced.

Teunissen formulated the baseline length constrained integer least-squares problem in [17] as

$$\min_{\boldsymbol{\xi},\boldsymbol{N}} \|\boldsymbol{\Psi} - \boldsymbol{H}\boldsymbol{\xi} - \boldsymbol{A}\boldsymbol{N}\|^2_{\boldsymbol{\Sigma}^{-1}}, \quad \boldsymbol{\xi} \in \mathbb{R}^3, \quad \boldsymbol{N} \in \mathbb{Z}^K, \quad \text{s.t.} \quad \|\boldsymbol{\xi}\| = l. \tag{5.1}$$

The baseline is reparameterized in spherical coordinates, i.e.

$$\boldsymbol{\xi}(\boldsymbol{\gamma}) = l \begin{bmatrix} \cos(\alpha)\cos(\beta) \\ \cos(\alpha)\sin(\beta) \\ \sin(\alpha) \end{bmatrix} \quad \text{with} \quad \boldsymbol{\gamma} = \begin{bmatrix} \alpha \\ \beta \end{bmatrix}, \tag{5.2}$$

and, thus, (5.1) can be written as unconstrained equation

$$\min_{\boldsymbol{\gamma},\boldsymbol{N}} \|\boldsymbol{\Psi} - \boldsymbol{H}\boldsymbol{\xi}(\boldsymbol{\gamma}) - \boldsymbol{A}\boldsymbol{N}\|^2_{\boldsymbol{\Sigma}^{-1}}, \quad \boldsymbol{\gamma} \in \mathbb{R}^2, \quad \boldsymbol{N} \in \mathbb{Z}^K, \tag{5.3}$$

which is nonlinear in $\boldsymbol{\gamma}$. Linearization of the baseline vector with respect to some approximated angles $\boldsymbol{\gamma}_0 = \begin{bmatrix} \alpha_0 & \beta_0 \end{bmatrix}^T$ gives

$$\boldsymbol{\xi}(\boldsymbol{\gamma}) = \boldsymbol{\xi}(\boldsymbol{\gamma}_0) + \boldsymbol{C}(\boldsymbol{\gamma}_0)\boldsymbol{\Delta\gamma} \tag{5.4}$$

with

$$\boldsymbol{C}(\boldsymbol{\gamma}_0) = l \begin{bmatrix} -\sin(\alpha_0)\cos(\beta_0) & -\cos(\alpha_0)\sin(\beta_0) \\ -\sin(\alpha_0)\sin(\beta_0) & \cos(\alpha_0)\cos(\beta_0) \\ \cos(\alpha_0) & 0 \end{bmatrix} \tag{5.5}$$

and $\boldsymbol{\Delta\gamma} = \boldsymbol{\gamma} - \boldsymbol{\gamma}_0$. Substituting $\boldsymbol{\xi}(\boldsymbol{\gamma})$ in (5.3) by (5.4) gives an unconstrained, linearized integer least-squares problem:

$$\min_{\boldsymbol{\Delta\gamma},\boldsymbol{N}} \|\boldsymbol{\Delta\Psi} - \boldsymbol{HC}(\boldsymbol{\gamma}_0)\boldsymbol{\Delta\gamma} - \boldsymbol{AN}\|^2_{\boldsymbol{\Sigma}^{-1}}, \quad \boldsymbol{\Delta\gamma} \in \mathbb{R}^2, \quad \boldsymbol{N} \in \mathbb{Z}^K, \tag{5.6}$$

with $\boldsymbol{\Delta\Psi} = \boldsymbol{\Psi} - \boldsymbol{H\xi}(\boldsymbol{\gamma}_0)$. Equation (5.6) is a linearized minimization problem which has the same structure as the integer least-squares problem without the baseline a priori information. Therefore, (5.6) can be solved by using the well known LAMBDA method. The approximate angles $\boldsymbol{\gamma}_0$ can be obtained from an external attitude determination method (IMU) or from float solution. However, in the latter case, the estimation of $\boldsymbol{\gamma}_0$ requires a large number of epochs for very small baselines.

Now, we introduce two new methods that make use of the integer least-square procedures discussed in previous chapters to reduce the search space to a certain extend, but to have a defined number of candidates left for the following integer ambiguity resolution. The advantage of this procedure is the possibility to choose the correct ambiguity vector even in case of incorrect determination of the ambiguity vector with the classical LAMBDA method. Fig. (5.1) illustrates that classical integer least square method is

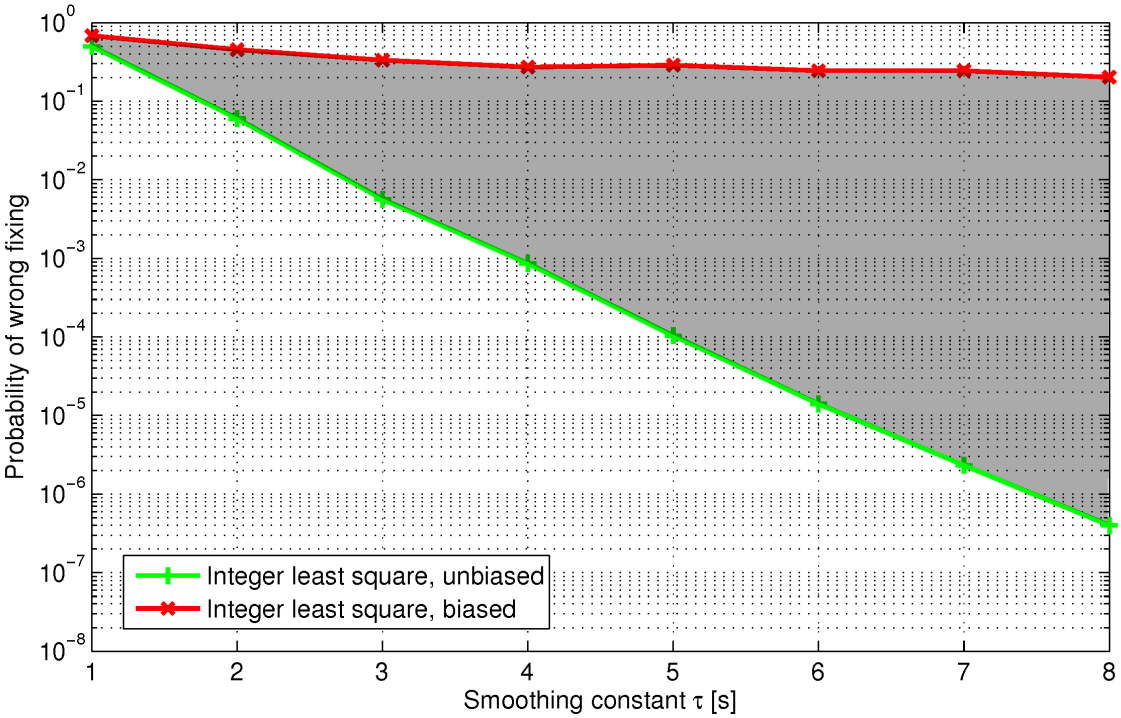

Figure 5.1: Classical integer least square method is sensitive concerning biases. The gray shaded area indicates the large space of probability of wrong fixing if the magnitude of bias error in measurement is not known.

quite sensitive in presence of biases. Starting point for both new methods is the set

of candidates of ambiguity vectors delivered from the previous mentioned integer least square method, which can yet be constrained on a priori information. This set of candidates defines our new search space.

5.1 Tightly constrained ambiguity resolution

Now we introduce our new method for the case of known baseline length l

$$\min_{\boldsymbol{\xi}(\boldsymbol{N})} \left\|\check{\boldsymbol{\xi}}\left(\boldsymbol{N}\right)-\boldsymbol{\xi}(\boldsymbol{N})\right\|^2_{\boldsymbol{\Sigma}^{-1}_{\check{\boldsymbol{\xi}}(\boldsymbol{N})}} \quad \longrightarrow \quad \min_{\boldsymbol{\xi}(\boldsymbol{N}),\|\boldsymbol{\xi}(\boldsymbol{N})\|=l} \left\|\check{\boldsymbol{\xi}}\left(\boldsymbol{N}\right)-\boldsymbol{\xi}(\boldsymbol{N})\right\|^2_{\boldsymbol{\Sigma}^{-1}_{\check{\boldsymbol{\xi}}(\boldsymbol{N})}}. \tag{5.7}$$

The well known Lagrange method is used to constrain the baseline to a fixed length. This is done by adding a term that evaluates to zero.

$$\begin{aligned} f(\lambda,\boldsymbol{N}) := \left\|\check{\boldsymbol{\xi}}\left(\boldsymbol{N}\right)-\boldsymbol{\xi}(\boldsymbol{N})\right\|^2_{\boldsymbol{\Sigma}^{-1}_{\check{\boldsymbol{\xi}}(\boldsymbol{N})}} &= \left(\check{\boldsymbol{\xi}}\left(\boldsymbol{N}\right)-\boldsymbol{\xi}(\boldsymbol{N})\right)^T \boldsymbol{\Sigma}^{-1}_{\check{\boldsymbol{\xi}}(\boldsymbol{N})} \left(\check{\boldsymbol{\xi}}\left(\boldsymbol{N}\right)-\boldsymbol{\xi}(\boldsymbol{N})\right) \\ &\quad + \underbrace{\lambda(\boldsymbol{\xi}^T(\boldsymbol{N})\boldsymbol{\xi}(\boldsymbol{N})-l^2)}_{=0}. \end{aligned} \tag{5.8}$$

Computing the derivative of $f(\lambda,\boldsymbol{N})$ with respect to $\boldsymbol{\xi}$ gives

$$\frac{df(\lambda,\boldsymbol{N})}{d\boldsymbol{\xi}} = \boldsymbol{\Sigma}^{-1}_{\check{\boldsymbol{\xi}}(\boldsymbol{N})}\left(\boldsymbol{\xi}(\boldsymbol{N})-\check{\boldsymbol{\xi}}\left(\boldsymbol{N}\right)\right)+\lambda\boldsymbol{\xi}(\boldsymbol{N}). \tag{5.9}$$

Setting the derivative equal to zero gives

$$\frac{df(\lambda,\boldsymbol{N})}{d\boldsymbol{\xi}} \stackrel{!}{=} 0 \qquad \Leftrightarrow \qquad \boldsymbol{\xi}(\boldsymbol{N}) = \left(\boldsymbol{\Sigma}^{-1}_{\check{\boldsymbol{\xi}}(\boldsymbol{N})}-\lambda\mathbf{1}\right)^{-1}\boldsymbol{\Sigma}^{-1}_{\check{\boldsymbol{\xi}}(\boldsymbol{N})}\check{\boldsymbol{\xi}}\left(\boldsymbol{N}\right) \tag{5.10}$$

and with the constrained $\|\boldsymbol{\xi}(\boldsymbol{N})\|^2 = l^2$ we get

$$\check{\boldsymbol{\xi}}^T(\boldsymbol{N})\boldsymbol{\Sigma}^{-1}_{\check{\boldsymbol{\xi}}(\boldsymbol{N})}\left(\boldsymbol{\Sigma}^{-1}_{\check{\boldsymbol{\xi}}(\boldsymbol{N})}-\lambda\mathbf{1}\right)^{-1}\left(\boldsymbol{\Sigma}^{-1}_{\check{\boldsymbol{\xi}}(\boldsymbol{N})}-\lambda\mathbf{1}\right)^{-1}\boldsymbol{\Sigma}^{-1}_{\check{\boldsymbol{\xi}}(\boldsymbol{N})}\check{\boldsymbol{\xi}}\left(\boldsymbol{N}\right)-l^2=0. \tag{5.11}$$

Now, this equation has to be solved for λ but due to its high non-linearity it can not be solved analytically. However, the iterative Newton method provides an efficient method for the computation of λ. Therefore, we consider (5.11) as a function whose roots have to be determined, i.e.

$$f(\lambda) = \check{\boldsymbol{\xi}}^T(\boldsymbol{N})\boldsymbol{\Sigma}^{-1}_{\check{\boldsymbol{\xi}}(\boldsymbol{N})}\left(\boldsymbol{\Sigma}^{-1}_{\check{\boldsymbol{\xi}}(\boldsymbol{N})}-\lambda\mathbf{1}\right)^{-2}\boldsymbol{\Sigma}^{-1}_{\check{\boldsymbol{\xi}}(\boldsymbol{N})}\check{\boldsymbol{\xi}}\left(\boldsymbol{N}\right)-l^2 \stackrel{!}{=} 0, \tag{5.12}$$

where we simplified notation by defining

$$\left(\boldsymbol{\Sigma}^{-1}_{\check{\boldsymbol{\xi}}(\boldsymbol{N})}-\lambda\mathbf{1}\right)^{-2} = \left(\boldsymbol{\Sigma}^{-1}_{\check{\boldsymbol{\xi}}(\boldsymbol{N})}-\lambda\mathbf{1}\right)^{-1}\left(\boldsymbol{\Sigma}^{-1}_{\check{\boldsymbol{\xi}}(\boldsymbol{N})}-\lambda\mathbf{1}\right)^{-1}. \tag{5.13}$$

The application of the Newton method (appendix) requires the computation of the derivative with respect to λ, i.e.

$$A(\lambda) := \frac{df(\lambda)}{d\lambda} = 2\cdot\check{\boldsymbol{\xi}}^T(\boldsymbol{N})\boldsymbol{\Sigma}^{-1}_{\check{\boldsymbol{\xi}}(\boldsymbol{N})}\left(\boldsymbol{\Sigma}^{-1}_{\check{\boldsymbol{\xi}}(\boldsymbol{N})}-\lambda\mathbf{1}\right)^{-3}\boldsymbol{\Sigma}^{-1}_{\check{\boldsymbol{\xi}}(\boldsymbol{N})}\check{\boldsymbol{\xi}}\left(\boldsymbol{N}\right). \tag{5.14}$$

By now, where $f(\lambda)$ and $A(\lambda)$ are defined the iterative prescription for computing λ is

$$\lambda_{n+1} = \lambda_n + A^{-1}(\lambda_n) \cdot f(\lambda_n). \tag{5.15}$$

The iterative computation needs an initial value λ_0 which is known to be a rather uncritical choice using the Newton algorithm. In the context of ambiguity resolution, $\lambda_0 = 0$ corresponds to the unconstrained integer least-squares estimation, which serves as a good starting point. There is always the possibility to check the resulting λ for correctness by simply checking if

$$|f(\lambda)| < \epsilon \tag{5.16}$$

holds true. (5.16) is equivalent to $f(\lambda) \approx 0$ and is assumed to approximately meet the requirement of equation (5.12) where ϵ denotes a constant near zero that has to be used due to the presence of small numerical errors and to give the possibility to trade between accuracy and computational effort. Furthermore, this check can be used as stop criterion for the numerical determination of λ. In all analysis and simulations mentioned in this thesis, $\epsilon = 10^{-7}$ was the choice for the stop criterion. Experience has shown that the Newton algorithm is well tempered even with respect to speed of convergence. In most of the cases, $\epsilon = 10^{-7}$ was fulfilled in much less than 30 iterations.

5.2 Loosely constrained ambiguity resolution

In the previous section we discussed how to use the information about the baseline length to reduce the probability of wrong ambiguity fixing. Therefore, we used the Lagrange method which constrains the baseline to a tightly fixed length. This method works well if the baseline length is exactly known. But in general the baseline length can not be measured exactly or diverges from assumed length. Hence there is always a variance in the baseline length.

The tightly constrained method is rather sensitive in this regard. The reason is the hard condition of the Lagrange method to find a baseline which fulfills the a priori knowledge in an exact sense. That leads to a high probability of wrong fixing in the case of an erroneous a priori knowledge.

In this section, a new loosely constrained method is introduced that shows a substantial robustness over errors in the assumed baseline length. Therefore, we define a new cost function

$$J(\boldsymbol{\xi}, \mu) = \mu \sum_{i=1}^{M} \left(\left\| \tilde{\boldsymbol{\xi}}(t_i) \right\| - l \right)^2 + \| \Delta \nabla \boldsymbol{\lambda\phi} - \boldsymbol{H\xi} - \boldsymbol{AN} \|^2_{\boldsymbol{\Sigma}^{-1}}, \tag{5.17}$$

where the confidence factor μ shall be chosen according to the expected accuracy of assumed baseline length. A high value of μ denote a high confidence in the a priori knowledge, while a low μ denotes a small confidence in the a priori knowledge. Note that

both squares in (5.17) ensure a positiv accumulation of the errors. The cost function (5.17) degrades to

$$J(\boldsymbol{\xi},\mu) = \sum_{i=1}^{M} \left(\left\| \tilde{\boldsymbol{\xi}}(t_i) \right\| - l \right)^2 \quad \text{with} \quad \mu \to \infty, \tag{5.18}$$

which is equivalent to the tightly constrained ambiguity resolution method in statistical average. On the other hand the cost function (5.17) degrades to

$$J(\boldsymbol{\xi},\mu) = \|\Delta\nabla\boldsymbol{\lambda}\boldsymbol{\phi} - \boldsymbol{H}\boldsymbol{\xi} - \boldsymbol{A}\boldsymbol{N}\|^2_{\boldsymbol{\Sigma}^{-1}} \quad \text{with} \quad \mu = 0, \tag{5.19}$$

which is identical to the unconstrained standard least square solution. Setting μ to any value between 0 and infinity provides the baseline constrained ambiguity resolution method with a knowledge about the variance of assumed baseline length with any value between "no trust" and "full trust". E.g. in the application of helicopter load transportation, where the rope is equivalent to the known baseline as shown in [3] and [4] μ is adapted to the specific modulus of elasticity of the rope and weight of the load.

The common way in computing the cost function (5.17) would be to use all available epochs of measurements in a block vector and matrix notation.

$$\boldsymbol{\Psi} = \begin{bmatrix} \tilde{\boldsymbol{\Psi}}(t_1) \\ \tilde{\boldsymbol{\Psi}}(t_2) \\ \vdots \\ \tilde{\boldsymbol{\Psi}}(t_M) \end{bmatrix}, \qquad \boldsymbol{H} = \begin{bmatrix} \tilde{\boldsymbol{H}}(t_1) & & & \\ & \tilde{\boldsymbol{H}}(t_2) & & \\ & & \ddots & \\ & & & \tilde{\boldsymbol{H}}(t_M) \end{bmatrix},$$

$$\boldsymbol{\xi} = \begin{bmatrix} \tilde{\boldsymbol{\xi}}(t_1) \\ \tilde{\boldsymbol{\xi}}(t_2) \\ \vdots \\ \tilde{\boldsymbol{\xi}}(t_M) \end{bmatrix}, \qquad \boldsymbol{\Sigma}^{-1} = \begin{bmatrix} \tilde{\boldsymbol{\Sigma}}^{-1}(t_1) & & & \\ & \tilde{\boldsymbol{\Sigma}}^{-1}(t_2) & & \\ & & \ddots & \\ & & & \tilde{\boldsymbol{\Sigma}}^{-1}(t_M) \end{bmatrix}.$$

With this variables and the definition

$$\boldsymbol{\Psi} = \Delta\nabla\boldsymbol{\lambda}\boldsymbol{\phi} - \boldsymbol{A}\boldsymbol{N} \tag{5.20}$$

the second term of equation (5.17) can be written as

$$\begin{aligned}
&(\boldsymbol{\Psi} - \boldsymbol{H}\boldsymbol{\xi})^T \boldsymbol{\Sigma} (\boldsymbol{\Psi} - \boldsymbol{H}\boldsymbol{\xi}) \\
&= \left(\tilde{\boldsymbol{\Psi}}(t_1) - \tilde{\boldsymbol{H}}(t_1)\tilde{\boldsymbol{\xi}}(t_1)\right)^T \tilde{\boldsymbol{\Sigma}}^{-1}(t_1) \left(\tilde{\boldsymbol{\Psi}}(t_1) - \tilde{\boldsymbol{H}}(t_1)\tilde{\boldsymbol{\xi}}(t_1)\right) \\
&\quad + \left(\tilde{\boldsymbol{\Psi}}(t_2) - \tilde{\boldsymbol{H}}(t_2)\tilde{\boldsymbol{\xi}}(t_2)\right)^T \tilde{\boldsymbol{\Sigma}}^{-1}(t_2) \left(\tilde{\boldsymbol{\Psi}}(t_2) - \tilde{\boldsymbol{H}}(t_2)\tilde{\boldsymbol{\xi}}(t_2)\right) \\
&\quad + \cdots \\
&\quad + \left(\tilde{\boldsymbol{\Psi}}(t_M) - \tilde{\boldsymbol{H}}(t_M)\tilde{\boldsymbol{\xi}}(t_M)\right)^T \tilde{\boldsymbol{\Sigma}}^{-1}(t_M) \left(\tilde{\boldsymbol{\Psi}}(t_M) - \tilde{\boldsymbol{H}}(t_M)\tilde{\boldsymbol{\xi}}(t_M)\right)
\end{aligned} \tag{5.21}$$

which can be interpreted as sum of cost over all available epochs. This equation is obviously valid for single and multiple epochs. From these definitions it can be shown why the first term of cost function (5.17) must be written as sum over squared differences. In the case of using a single epoch (5.17) can be rewritten to

$$J(\boldsymbol{\xi},\mu) = \mu\left(\|\boldsymbol{\xi}\| - l\right)^2 + \|\Delta\nabla\boldsymbol{\lambda\phi} - \boldsymbol{H\xi} - \boldsymbol{AN}\|^2_{\boldsymbol{\Sigma}^{-1}} \quad \text{with} \quad \boldsymbol{\xi} = \tilde{\boldsymbol{\xi}}(t_1). \tag{5.22}$$

But setting a multi epoch $\boldsymbol{\xi}$ i.e. $M > 1$ into the first term would lead to

$$\mu\left(\|\boldsymbol{\xi}\| - l\right)^2 = \mu\left(\sqrt{\tilde{\boldsymbol{\xi}}^T(t_1)\tilde{\boldsymbol{\xi}}(t_1) + \tilde{\boldsymbol{\xi}}^T(t_2)\tilde{\boldsymbol{\xi}}(t_2) + \cdots + \tilde{\boldsymbol{\xi}}^T(t_M)\tilde{\boldsymbol{\xi}}(t_M)} - l\right)^2 \tag{5.23}$$

which is not a sum of cost over all available epochs. The correct expression for a sum of cost over multiple epochs is

$$\begin{aligned}\mu\Bigg[&\left(\sqrt{\tilde{\boldsymbol{\xi}}^T(t_1)\tilde{\boldsymbol{\xi}}(t_1)} - l\right)^2 + \left(\sqrt{\tilde{\boldsymbol{\xi}}^T(t_2)\tilde{\boldsymbol{\xi}}(t_2)} - l\right)^2 + \cdots \\ &+ \left(\sqrt{\tilde{\boldsymbol{\xi}}^T(t_M)\tilde{\boldsymbol{\xi}}(t_M)} - l\right)^2\Bigg] = \mu\sum_{i=1}^{M}\left(\left\|\tilde{\boldsymbol{\xi}}(t_i)\right\| - l\right)^2.\end{aligned} \tag{5.24}$$

Therefore expression (5.24) is used as first term in (5.17).

Now, we rewrite cost function (5.17) as

$$J(\boldsymbol{\xi},\mu) = \mu\sum_{i=1}^{M}\left(\sqrt{\tilde{\boldsymbol{\xi}}_i^T\tilde{\boldsymbol{\xi}}_i} - l\right)^2 + \|\boldsymbol{\Psi} - \boldsymbol{H\xi}\|^2_{\boldsymbol{\Sigma}^{-1}} \tag{5.25}$$

$$\begin{aligned}&= \mu\sum_{i=1}^{M}\left(\sqrt{\tilde{\boldsymbol{\xi}}_i^T\tilde{\boldsymbol{\xi}}_i} - l\right)^2 + \left(\boldsymbol{\Psi} - \boldsymbol{H\xi}\right)^T\boldsymbol{\Sigma}^{-1}\left(\boldsymbol{\Psi} - \boldsymbol{H\xi}\right) \\ &= \mu\sum_{i=1}^{M}\left(\sqrt{\tilde{\boldsymbol{\xi}}_i^T\tilde{\boldsymbol{\xi}}_i} - l\right)^2 + \boldsymbol{\Psi}^T\boldsymbol{\Sigma}^{-1}\boldsymbol{\Psi} - \boldsymbol{\xi}^T\boldsymbol{H}^T\boldsymbol{\Sigma}^{-1}\boldsymbol{\Psi} \\ &\quad - \boldsymbol{\Psi}^T\boldsymbol{\Sigma}^{-1}\boldsymbol{H\xi} + \boldsymbol{\xi}^T\boldsymbol{H}^T\boldsymbol{\Sigma}^{-1}\boldsymbol{H\xi}.\end{aligned} \tag{5.26}$$

Minimizing (5.25) over $\boldsymbol{\xi}$ leads to the derivative

$$f(\boldsymbol{\xi}) = \frac{dJ(\boldsymbol{\xi})}{d\boldsymbol{\xi}} = 2\mu\cdot\sum_{i=1}^{M}\frac{\tilde{\boldsymbol{\xi}}_i}{\left\|\tilde{\boldsymbol{\xi}}_i\right\|}\left(\left\|\tilde{\boldsymbol{\xi}}_i\right\| - l\right) - 2\boldsymbol{H}^T\boldsymbol{\Sigma}^{-1}\boldsymbol{\Psi} + 2\boldsymbol{H}^T\boldsymbol{\Sigma}^{-1}\boldsymbol{H\xi} \stackrel{!}{=} 0. \tag{5.27}$$

Due to the high non-linearity of (5.27), it is not possible to solve for the baseline $\boldsymbol{\xi}$ directly. As in the previous section, we will search for the root of equation (5.27) with the well known Newton method. Writing (5.27) as Taylor series gives us

$$f(\boldsymbol{\xi} + \Delta\boldsymbol{\xi}) = f(\boldsymbol{\xi}) + \frac{df(\boldsymbol{\xi})}{d\boldsymbol{\xi}}\cdot\Delta\boldsymbol{\xi} + R(\Delta\boldsymbol{\xi}^2). \tag{5.28}$$

The remainder $R(\Delta\boldsymbol{\xi}^2)$ is small compared to the first two terms so we will neglect it in the following:

$$f(\boldsymbol{\xi} + \Delta\boldsymbol{\xi}) = f(\boldsymbol{\xi}) + \frac{df(\boldsymbol{\xi})}{d\boldsymbol{\xi}} \cdot \Delta\boldsymbol{\xi}. \tag{5.29}$$

Solving this equation for $\Delta\boldsymbol{\xi}$ gives us

$$\Delta\boldsymbol{\xi} = -\left(\frac{df(\boldsymbol{\xi})}{d\boldsymbol{\xi}}\right)^{-1} \cdot f(\boldsymbol{\xi}). \tag{5.30}$$

With

$$\boldsymbol{\xi}_{n+1} = \boldsymbol{\xi}_n + \Delta\boldsymbol{\xi} \tag{5.31}$$

we can write

$$\boldsymbol{\xi}_{n+1} = \boldsymbol{\xi}_n - \left(\frac{df(\boldsymbol{\xi})}{d\boldsymbol{\xi}}\right)^{-1} \cdot f(\boldsymbol{\xi}) \tag{5.32}$$

Computing the derivative

$$\boldsymbol{A}(\boldsymbol{\xi}) = \frac{df(\boldsymbol{\xi})}{d\boldsymbol{\xi}} = 2\mu \sum_{i=1}^{M} \left(\mathbf{1} - l \left(\mathbf{1} \frac{1}{\left\| \tilde{\boldsymbol{\xi}}_i \right\|} - \frac{\tilde{\boldsymbol{\xi}}_i \tilde{\boldsymbol{\xi}}_i^T}{\left\| \tilde{\boldsymbol{\xi}}_i \right\|^3} \right) \right) + 2\boldsymbol{H}^T \boldsymbol{\Sigma}^{-1} \boldsymbol{H} \tag{5.33}$$

finally leads to

$$\boldsymbol{\xi}_{n+1} = \boldsymbol{\xi}_n - \boldsymbol{A}^{-1}(\boldsymbol{\xi}_n) \cdot \boldsymbol{f}(\boldsymbol{\xi}_n), \tag{5.34}$$

which is an iterative prescription to compute the $\boldsymbol{\xi}$ that solves equation (5.27) and thus is the baseline that minimizes the cost function (5.25).

The iterative computation needs an initial baseline $\boldsymbol{\xi}_0$ which is known to be a rather uncritical choice using the Newton algorithm. Even more if an initial baseline is chosen that meet the constraint on baseline length. Actually, an initialisation with $\boldsymbol{\xi}_0 = l \cdot \mathbf{1}$ appeared to be uncritical in all simulations. Moreover in some applications there is already a knowledge about the rough attitude of the baseline vector e.g. a sling load attached to a helicopter where the baseline is equivalent to the rope would roughly point in direction of earth centre due to gravitation.

6 Results

The benefit of the tight and soft constrained integer ambiguity resolution techniques is analyzed for both simulated and "real" Galileo measurements in this chapter. The PolaRx3G receiver of Septentrio was used to track the Galileo measurements provided by the high frequency signal simulator. The results show a dramatic improvement in the probability of wrong fixing.

6.1 Simulation results

Phase only measurements were used to avoid code multipath. Double differenced measurements were used to eliminate both receiver and satellite biases. A dual frequency widelane combination of E1 and E5a measurements was used to increase the carrier wavelength from 19.0cm and 25.5cm to 75.1cm. The phase noise was assumed to be Gaussian distributed with a standard deviation of 2mm. The elevation mask was set to 5 degrees.

Our model for the double difference (DD) measurements includes a simulation of the true DD ranges, the DD integer ambiguities, the DD zero-mean Gaussian distributed phase noises and the DD phase multipaths. The DD ranges were obtained from the Galileo satellite positions (described by the 27/3/1 Walker constellation), the position of the reference station and a certain baseline vector. The DD phase multipath delays were obtained from simulated undifferenced multipath delays, which were generated from a Gaussian distribution with an elevation dependent standard deviation.

The generation of measurements at multiple epochs is straightforward: the double difference ranges are adapted according to the orbital description, the phase noise is assumed to be statistically independent between epochs, the phase multipath is assumed to be fully temporary correlated (a worst-case scenario) over short periods, and the integer ambiguities are assumed to be constant, i.e. there are no cycle slips. For each satellite and each receiver, 10^8 statistically independent measurement noises and multipath delays were assumed.

Fig. (6.1) shows a comparison of the probability of wrong fixing of the unconstrained, the tightly constrained, and the soft constrained integer ambiguity resolution methods. The a priori information on the baseline length was assumed to be correct for both unconstrained and constrained ambiguity resolution. It was set to 30m. The confidence factor was set to $\mu = 1$. One can immediately observe that tightly and loosely constrained ambiguity resolution methods outperform unconstrained integer least squares estimation by several orders of magnitude, e.g. a benefit of 2 orders of magnitude is achieved after 4 epochs with 20 second intervals. The poorer performance of soft constrained ILS can be explained from the choice of μ: A value of $\mu = 1$ is not large enough to fully benefit

from the length a priori information.

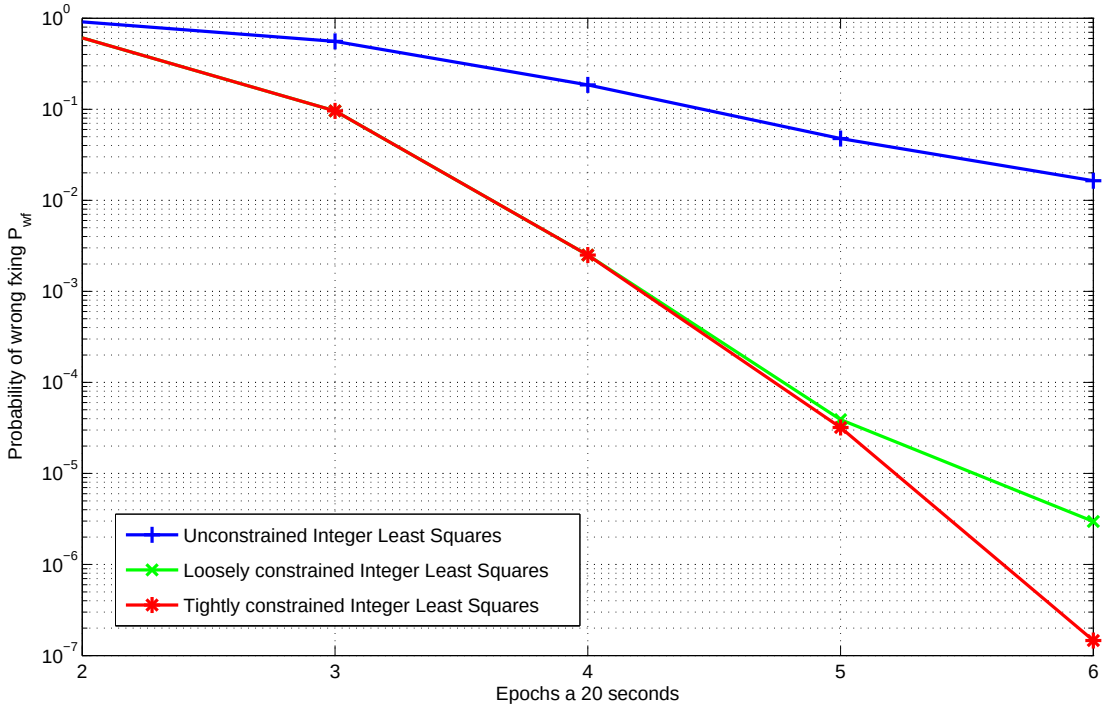

Figure 6.1: Benefit of constrained wide-lane integer ambiguity resolution over unconstrained wide-lane integer ambiguity resolution. The exact a priori knowledge of the baseline (tightly constrained) reduces the probability of wrong fixing by several orders of magnitude.

The effect of μ on the probability of wrong fixing is analyzed in Fig. (6.2). Here, an error in the a priori information was assumed, i.e. the a priori information was set to values between 20m and 38m while the correct length was 30m. The probability of wrong fixing was determined from Monte-Carlo simulations, and is shown over the assumed baseline length. Obviously, unconstrained ILS is independent of the a priori knowledge about the baseline. On the contrary, tightly constrained ILS is quite sensitive w.r.t. an erroneous a priori information.

Loosely constrained ILS is plotted with confidence factor μ as parameter. In case of biased a priori information about baseline length, loosely constrained ILS outperforms both the unconstrained and tightly constrained ILS, if the confidence factor μ is properly chosen. E.g. in the case of 29m as assumed baseline length and $\mu = 1$ the probability of wrong fixing is 10^{-4}, which is still more than one order lower than unconstrained ILS and where tightly constrained ILS is not usable due to high probability of wrong fixing. Looking at the plots with 27m as assumed baseline length, which is equivalent to an error of 10% regarding the true baseline length, it is observable that $\mu = 0.1$ would be

the best choice. Important to note is that loosely constrained ILS with $\mu = 0$ behaves like unconstrained ILS and with $\mu \to \infty$ it behaves like tightly constrained ILS. This was explained analytically in the previous chapter and was validated by simulations now. Note that a minimal probability of wrong fixing of about 10^{-4} at 30m is certainly a high value for many applications. Using more epochs will solve this problem as seen at Fig. (6.1) where the lowest achievable probability of wrong fixing is plotted over observation time.

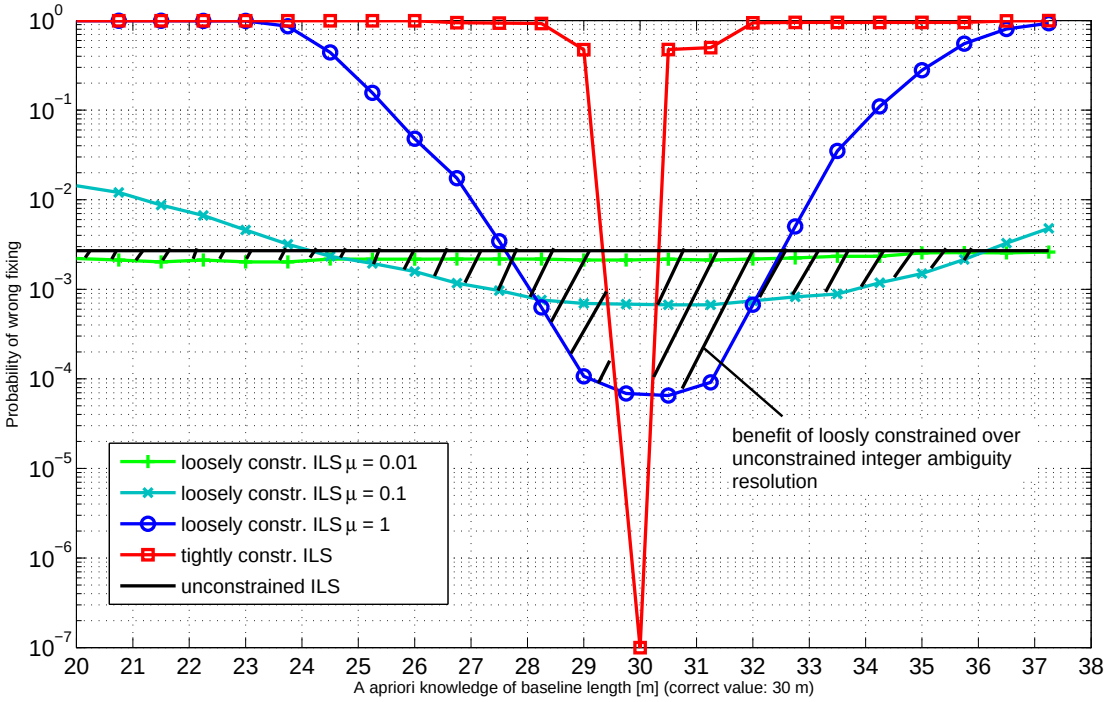

Figure 6.2: Benefit of a priori baseline knowledge: The loosely constrained ambiguity resolution outperforms both the unconstrained and the tightly constrained ambiguity resolution if the a priori knowledge is biased by a few percent. Parameters: 4 epochs à 200 seconds.

Now, we have a closer look at the previously mentioned probability of no candidate i.e. the probability that the true ambiguity vector is not present in the set of ambiguity vectors delivered by unconstrained ILS, and therefore is a lower bound on all constrained ILS methods that uses this set of integer ambiguity vectors as search space. In contrast to the previous simulation the following plots are computed with considering the influence of multipath on the measurements. This multipath was generated as random and Gaussian distributed noise, but with the property of adding the same multipath vector to all measurement epochs within a block (worst-case scenario). The standard deviation σ_{mp} was determined in dependence of the elevation of each satellite and the considered

	MP 1	MP 2	MP 3
$\left(\sigma_{\mathrm{mp}}^{90^\circ}\right)^2$	$1 \cdot 10^{-5}\mathrm{m}^2$	$4 \cdot 10^{-5}\mathrm{m}^2$	$1 \cdot 10^{-4}\mathrm{m}^2$
$\left(\sigma_{\mathrm{mp}}^{10^\circ}\right)^2$	$4 \cdot 10^{-5}\mathrm{m}^2$	$8 \cdot 10^{-5}\mathrm{m}^2$	$4 \cdot 10^{-4}\mathrm{m}^2$
$\sigma_{\mathrm{mp}}^{90^\circ}$	0.31cm	0.63cm	1.00cm
$\sigma_{\mathrm{mp}}^{10^\circ}$	0.63cm	0.89cm	2.00cm

Table 6.1: Definition and name of used multipath scenarios

magnitude:

$$\sigma_{\mathrm{mp}}(E) = \sigma_{\mathrm{mp}}^{10^\circ} \cdot e^{\frac{10^\circ - E}{\gamma}} \quad \text{with} \quad \gamma = \frac{80^\circ}{\ln \frac{\sigma_{\mathrm{mp}}^{10^\circ}}{\sigma_{\mathrm{mp}}^{90^\circ}}} \tag{6.1}$$

with E the elevation of the satellite in degree and $\sigma_{\mathrm{mp}}^{10^\circ}$, $\sigma_{\mathrm{mp}}^{90^\circ}$ the standard deviation of multipath defined at 10° respectively 90° elevation. Tab. (6.1) shows the variances and standard deviations used in each multipath scenario. The elevation was assumed to be constant due to the relative low number of epochs, therefore, the used standard deviation for multipath is listed in Tab. (6.2). In these simulations unconstrained ILS

Elevation	MP 1	MP 2	MP 3
30.1	0.53cm	0.82cm	1.68cm
66.0	0.39cm	0.70cm	1.23cm
43.7	0.47cm	0.77cm	1.50cm
07.3	0.65cm	0.90cm	2.05cm
29.6	0.53cm	0.82cm	1.69cm
52.0	0.44cm	0.75cm	1.39cm
07.3	0.65cm	0.91cm	2.05cm

Table 6.2: Standard deviation of artificial multipath used in simulations

was used to get a search space for the true ambiguity vector. In detail, this search space is a sorted list of ambiguity vectors where the first ambiguity vector in the list has the highest probability to be the true vector in the sense of unconstrained ILS. Fig. (6.3) shows the distribution of the position of the true integer ambiguity vector within this list. Classical unconstrained integer least square methods always take the first vector as estimated ambiguity vector. This can be cross-checked by looking at the unbiased probability of the first candidate to be the true one. With the probability of 0.95 as observed for unbiased probability for candidate 1 of Fig. (6.3), the probability of wrong fixing is $1 - 0.95 = 5 \cdot 10^{-2}$, which is exactly the value of unconstrained ILS in Fig. (6.1) with 5 epochs. Note that in the unbiased case the probability that the true ambiguity vector is on the tenth or higher position is no more visible in this figure. With growing magnitude of biases i.e. multipath on the measurements, certainly, the distribution

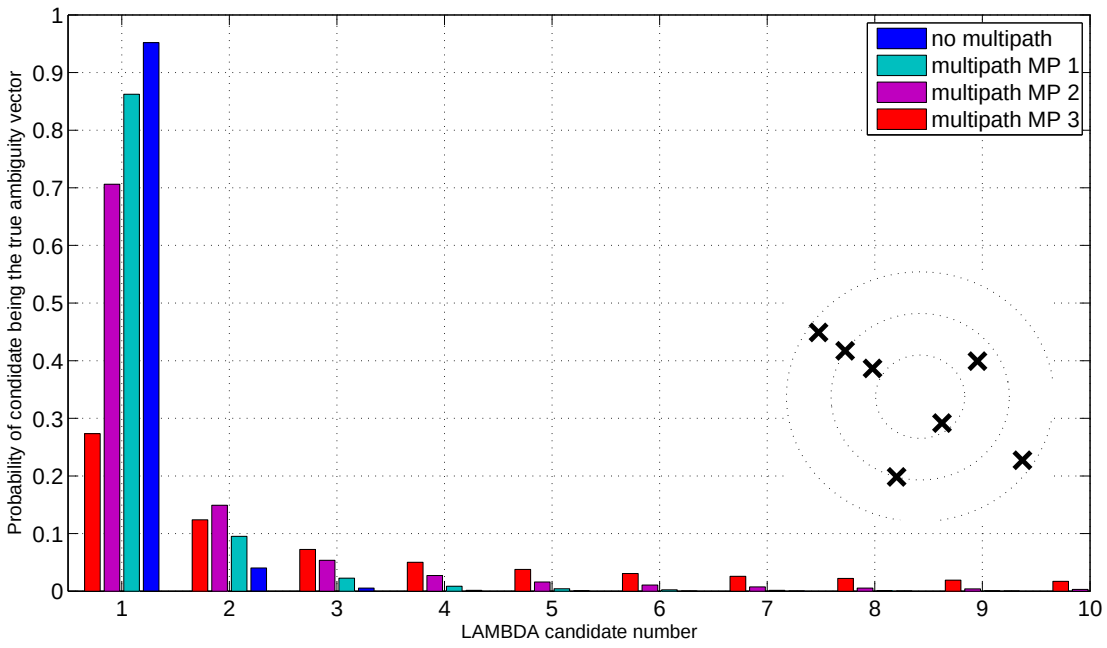

Figure 6.3: Distribution of the true ambiguity vector within list of sorted candidates supplied by LAMBDA. Parameters: 5 epochs à 20 seconds.

flattens which is equivalent to rising probability of higher true vector position. There has to be a predefined number of candidates which is equivalent to the length of sorted list for computing tightly and loosely constrained ambiguity resolution, due to restricted computation performance. Obviously, for constant number of candidates the probability of wrong fixing is rising with higher magnitude of multipath.

The probability of no candidate i.e. missing the true vector among the list of candidates, depending on the used number of candidates is plotted in Fig. (6.4) with magnitude of multipath as one parameter and number of epochs as second parameter. Rising the number of candidates always leads to a lower probability of no candidate, certainly. But with higher magnitude of multipath e.g. "MP 3" it is not efficient to further enlarge the number of candidates. Note that a number of candidates of 300 would mean an enormous computational effort due to the requirement of computing the whole (iterative) loosely or tightly constrained ambiguity resolution method for each candidate. Taking a longer observation time i.e. using more epochs leads to significant lower probability of no candidate in the case of low magnitude of multipath. E.g. the probability of no candidate with multipath "MP 1", 50 candidates and 4 epochs is $4 \cdot 10^{-4}$. Using one more epoch with 20 second leads to reduction of probability by more than 2 orders. Also note that this probability of no candidate is valid for not using a method for reducing the set of candidates with a priori knowledge about the baseline length as discussed in chapter 4. As discussed, the probability of no candidate is a lower bound on the probability of

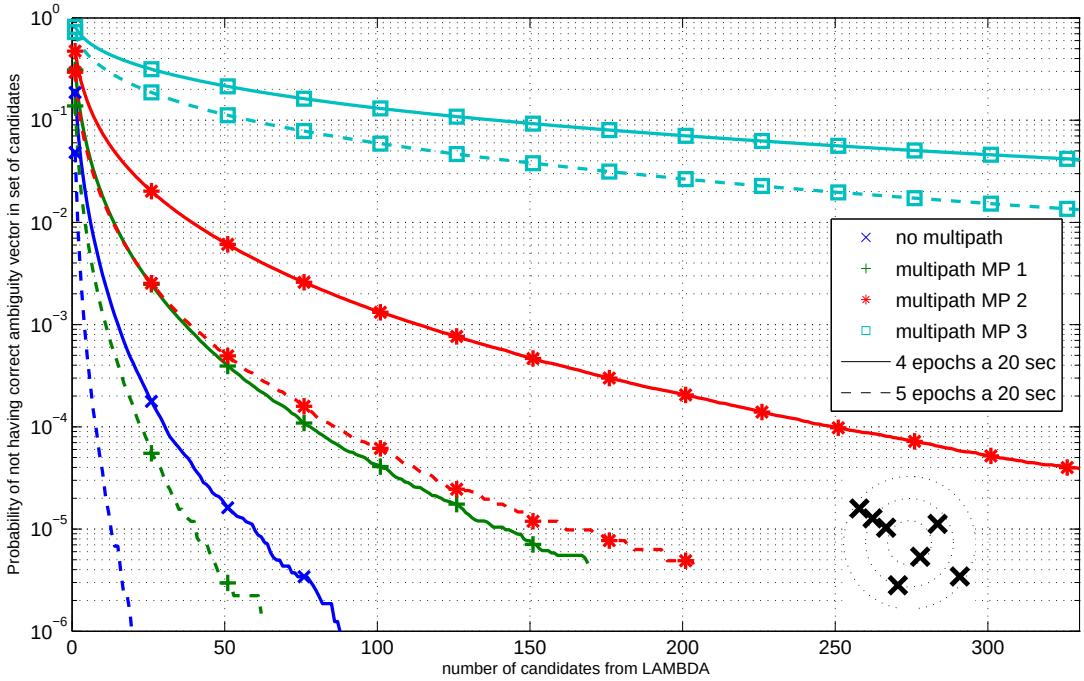

Figure 6.4: Influence of multipath and observation time on required number of candidates. In the case of not integrating the baseline constraints into LAMBDA the probability is equivalent to an upper bound on achievable performance.

wrong fixing for tightly and loosely ILS. Therefore, it is essential to achieve low probabilities of no candidate. The lowest probabilities of wrong fixing in Fig. (6.4) have a value about 10^{-6}. These probabilities are relatively high compared to requirements in many applications. The reason is the high computational effort for simulating probabilities lower than 10^{-6} where a block number of more than 10^8 would be necessary to achieve statistical validity. This computational problem is also the reason for the steps visible at lower probabilities.

In this thesis the main focus lies on reliability than on accuracy. However, performing simulations related to the baseline error vector is interesting regarding the influence of multipath and in cases of wrong fixing of the ambiguity vector. The baseline error vector is the difference between estimated baseline and true baseline. Fig. (6.5) shows the density of the norm of the baseline error vector, i.e. the density of the baseline error length for the tightly constrained ambiguity resolution method. E.g. the red bar at 2cm means that 45% of the baseline error vectors have a length in between 1cm and 2cm. The same simulation was performed for the loosely constrained ambiguity resolution method in Fig. (6.6). Note that the integral over each density function must be 1. For the blue curve, i.e. the highest simulated multipath, the integral over the visible range form

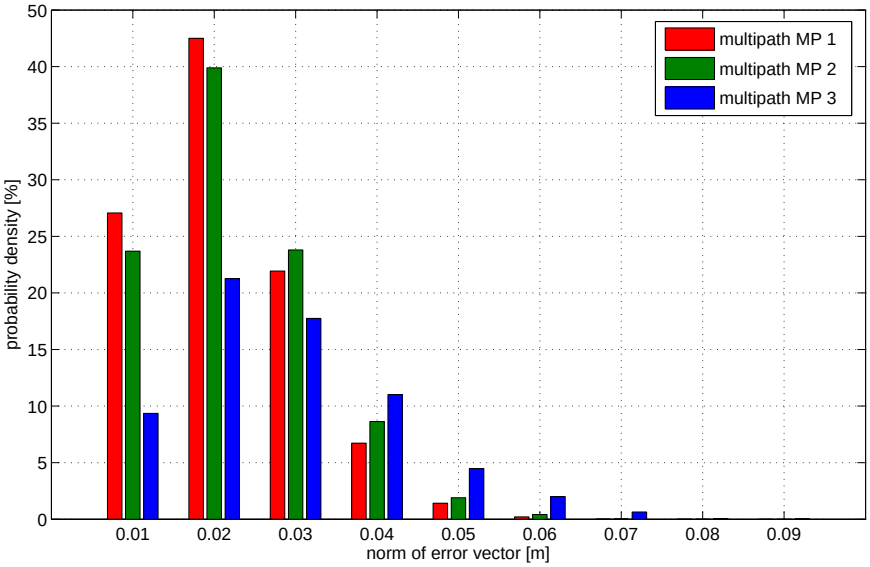

Figure 6.5: Tightly constrained ambiguity resolution method: Density of norm of baseline error vector with correct a priori baseline length.

0cm to 9cm is not 1. The reason is the high probability of wrong fixing achieved with this magnitude of multipath. In the case of wrong integer ambiguity fixing the length of the baseline error vector could be at the magnitude of the whole baseline length. E.g. a probability of wrong fixing of 0.5 in general leads to long error vectors in half of the cases. This is observable in the error vector density plots, where almost exclusively baseline estimates with correct integer ambiguity fixing are visible.

Fig. (6.7) shows the error distribution of the baseline error vector length. It is observable that for large multipath magnitude many error vectors are longer than 9cm due to the visible saturation of the curves. Of course, all distributions achieve 1 but with high probability of wrong fixing there are many error vectors with length beyond 10m and, therefore, are not visible in this plot.

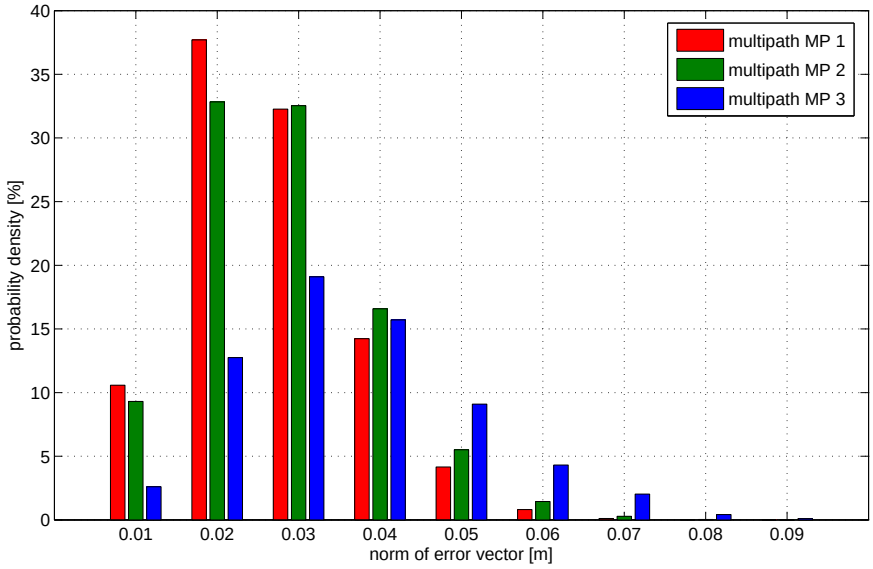

Figure 6.6: Loosely constrained ambiguity resolution method: Density of norm of baseline error vector with correct a priori baseline length and confidence factor $\mu = 1$.

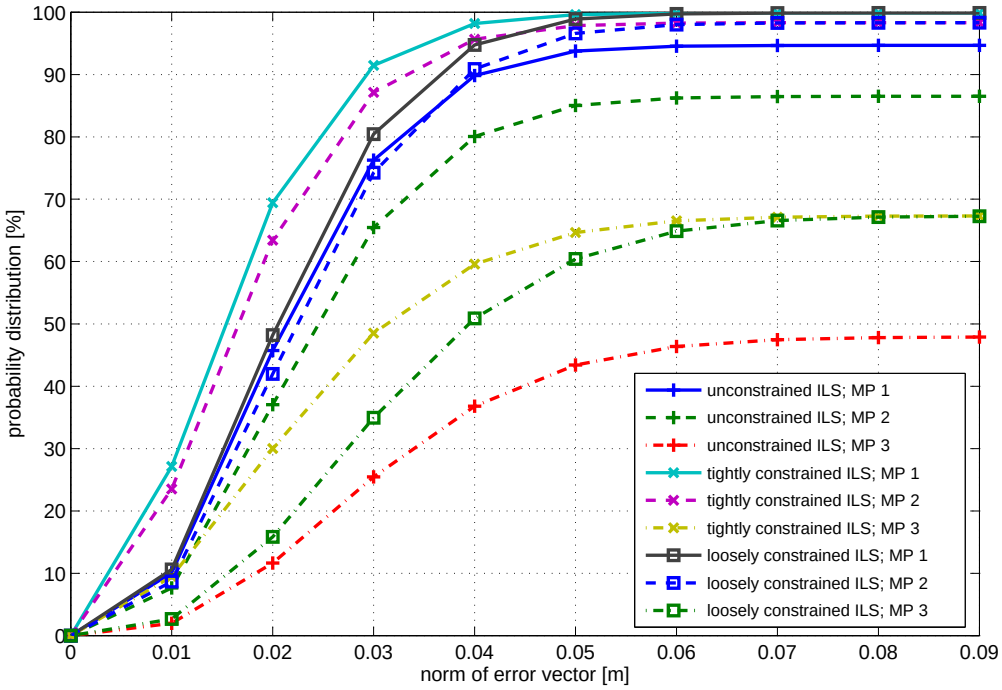

Figure 6.7: Distribution of norm of baseline error vector.

6.2 Measurement results

Measurements were performed with the equipment shown in Fig. (6.8). A Nav-X-NCS Galileo signal simulator of IFEN generated a Galileo constellation and made the antenna signal available at frequency E1 and E5a. This antenna signal is connected to a Septentrio PolaRx3G GPS/Galileo receiver, which logs the observation and navigation data in the Rinex 3.00 format. The used measurements had a duration of 31min with 9 satellites visible the whole time as shown in Fig. (6.9). The measurement was performed with

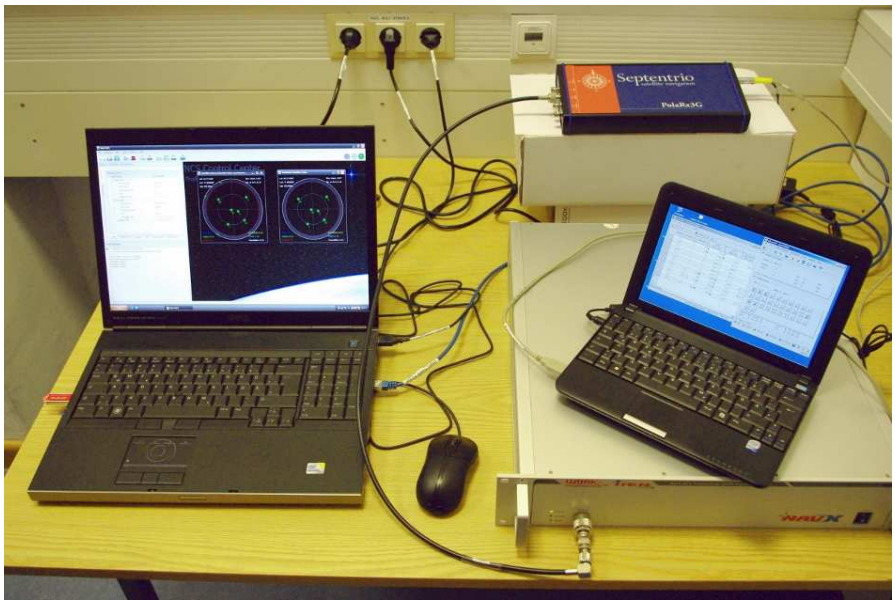

Figure 6.8: Measurement equipment: Nav-X-NCS Galileo signal simulator of IFEN is connected to a PolaRx3G GPS/Galileo receiver (E1, E5a/L5)

two different user positions for the same epoch. The distance between the two receivers is equivalent to the baseline and was adjusted to a length of 101.944m. Note that in contrast to simulations the true integer ambiguity vector is not known. Therefore, the focus for analysis of measurements lies on low residuals and low error in the baseline estimates.

Fig. (6.10) shows the length of baseline error vector over time. The code-only solution suffers from high noise. The code-carrier widelane combination, where the ambiguities are left float has a one order lower noise level than the code-only solution. Furthermore, fixing the ambiguities to integer values leads to millimetre noise level.

The high reliability in integer ambiguity fixing can be seen from Fig. (6.11). The float values of all 9 ambiguities are plotted over the observation time. Obviously all mean values of the ambiguities lies next to integer values and, therefore, can be easily fixed within a few epochs.

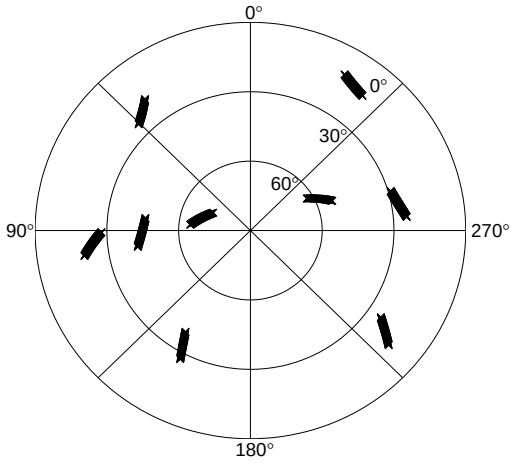

Figure 6.9: Skyplot of constellation generated by the Nav-X-NCS Galileo signal simulator. Date: 01.03.2010 12:00; Duration: 31 minutes

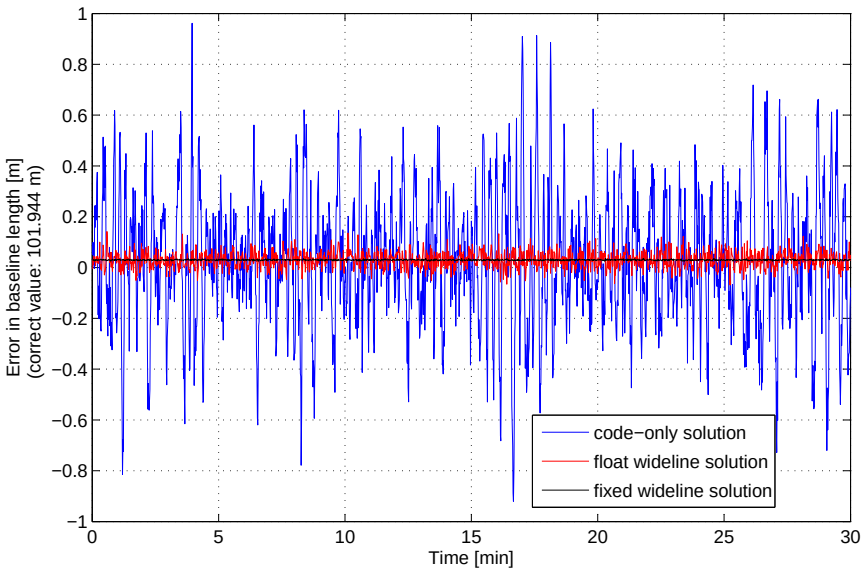

Figure 6.10: Length of baseline error vector: Fixing the ambiguities to integer values outperforms both the code-only solution and the code-carrier widelane combination where the ambiguities are left float.

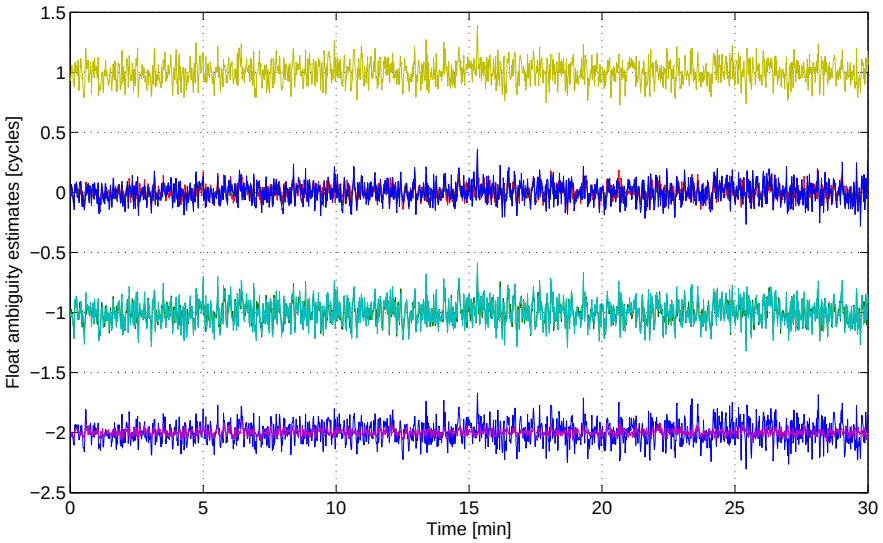

Figure 6.11: Float ambiguities over time: The not averaged ambiguity estimates are all next to integer values, which makes reliable integer fixing possible within a few epochs

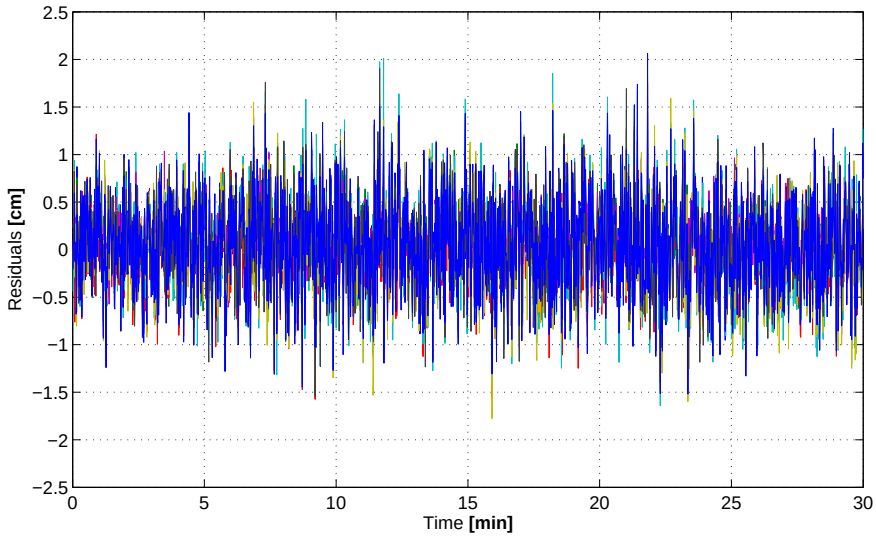

Figure 6.12: Pseudorange residuals: The difference between measured ranges and computed ranges has a magnitude of only a few centimetres

Fig. (6.12) illustrates the reliability of baseline estimate with showing the pseudorange residuals. These pseudorange residuals are the difference between measured ranges and computed ranges for all visible satellites. The magnitude of the residuals lies in the low centimetre level which also indicates a reliable baseline vector estimation.

7 Conclusion

In chapter 2, we derived optimal multi-frequency linear combinations with respect to ambiguity discrimination for improving the reliability of integer ambiguity resolution. The linear combination of code and phase measurements enable dual frequency widelane combinations that eliminate the ionospheric delay, which is not possible with phase-only combinations.

We discussed the well known LAMBDA method for integer least-square estimation and derived how to improve the search in the case of available a priori knowledge about the baseline length. Therefore, we introduced a check on the mixed float fixed ambiguity vectors which prevents the computing of ambiguity vectors that does not fulfill the constraint on baseline length. This leads to elimination of whole branches in the search tree, which reduces the computational effort for the search and, furthermore, it allows to extend the search space volume, which additionally lowers the probability of wrong fixing. In addition, it prevents the sequential shrinking of LAMBDA and, thereby, improves the search efficiency. Once the search tree is constructed, the ambiguity candidate vectors are a basis for the following integer ambiguity resolution methods.

Two new methods for integer ambiguity resolution with a priori information about the baseline length were derived in chapter 5. Both methods make use of the previously estimated candidate set of integer ambiguity vectors and the a priori information about the baseline length. First, we derived the tightly constrained ambiguity resolution method, which achieves several orders of magnitude lower probability of wrong fixing after a few epochs than unconstrained ambiguity resolution methods, but relies on high accuracy of knowledge about the priori baseline length. To cover the case of an error in a priori baseline length we, secondly, introduced the loosely constrained ambiguity resolution method, which takes the additional side information about the confidence of the assumed baseline length into account. Therefore, in the case of an error in a priori information, loosely constrained method outperforms both, unconstrained and tightly constrained ambiguity resolution. Furthermore, it has been demonstrated that substantial improvements of reliability of carrier phase positioning i.e. probability of correct fixing, were achieved as required in safety of life critical applications after a few epochs.

The introduced methods were first validated with simulations. It was shown that the probability of wrong fixing could be reduced by several orders of magnitude compared to unconstrained ambiguity resolution. A confidence factor was introduced for the a priori baseline length information, which is known only to a certain extent in most practical applications. The relevance of this confidence factor was confirmed, i.e. the loosely

constrained ambiguity resolution method clearly outperforms unconstrained and tightly constrained resolution methods. The norm of the baseline error lies in centimetre level in case of correct fixing.

In addition, "real" measurements were analyzed with the Septentrio PolaRx3G receiver, which was connected to the Galileo signal generator Nav-X-NCS of IFEN. The following observations were made for ambiguity resolution with an optimized code carrier E1-E5a widelane combination: first, the float ambiguity estimates converged to integer values. Secondly, the noise levels of the unfiltered float ambiguity estimates vary between one tenth and one third of the wavelength depending on the elevation of the satellites. This confirms the high reliability predicted by the ambiguity discrimination. Thirdly, the residuals for the fixed baseline solution were observed to be at the centimeter level.

Future work might include the introduction of further constraints, e.g. on the direction of the baseline. It is expected that this will further reduce the number of branches in the search tree, which enables an increased search space volume and, thus, a further reduction in the probability of wrong fixing. This could be important for a receiver environment with substantial multipath.

A Appendix

A.1 Multi-dimensional Newton algorithm

$$\begin{aligned} \boldsymbol{f}(\boldsymbol{e}_\xi) = l \cdot \boldsymbol{H}^T\boldsymbol{C}^{-1}\boldsymbol{H}\boldsymbol{e}_\xi + \boldsymbol{e}_\xi^T\boldsymbol{H}^T\boldsymbol{C}^{-1}\boldsymbol{\rho}\boldsymbol{H}^T\boldsymbol{C}^{-1}\boldsymbol{H}\boldsymbol{e}_\xi \\ -\boldsymbol{H}^T\boldsymbol{C}^{-1}\boldsymbol{\rho} - \boldsymbol{e}_\xi^T\boldsymbol{H}^T\boldsymbol{C}^{-1}\boldsymbol{H}\boldsymbol{e}_\xi\boldsymbol{H}^T\boldsymbol{C}^{-1}\boldsymbol{\rho} \end{aligned} \tag{A.1}$$

$$\boldsymbol{f}(\boldsymbol{x}) = \boldsymbol{y}_0 + \boldsymbol{A}(\boldsymbol{x} - \boldsymbol{x}_0) \text{ with the Jacobian } \quad \boldsymbol{A} = \begin{bmatrix} \frac{\delta y_1}{\delta x_1} & \cdots & \frac{\delta y_1}{\delta x_K} \\ \vdots & \ddots & \vdots \\ \frac{\delta y_K}{\delta x_1} & \cdots & \frac{\delta y_K}{\delta x_K} \end{bmatrix} \tag{A.2}$$

$$\boldsymbol{x} = \boldsymbol{x}_0 + \boldsymbol{A}^{-1}(\boldsymbol{y} - \boldsymbol{y}_0) \tag{A.3}$$

$$\underset{\boldsymbol{y}=\boldsymbol{0}}{=} \boldsymbol{x}_0 + \boldsymbol{A}^{-1}\boldsymbol{y}_0 \tag{A.4}$$

$\boldsymbol{f}(\boldsymbol{e}_\xi)$ is a vector (according to definition)
$\boldsymbol{A}$ consists of 4 terms

① $$\frac{\delta}{\delta \boldsymbol{e}_\xi}\left(l \cdot \boldsymbol{H}^T\boldsymbol{C}^{-1}\boldsymbol{H}\boldsymbol{e}_\xi\right) = l \cdot \boldsymbol{H}^T\boldsymbol{C}^{-1}\boldsymbol{H} \tag{A.5}$$

② $$\frac{\delta}{\delta \boldsymbol{e}_\xi}\left(\boldsymbol{e}_\xi^T \underbrace{\boldsymbol{H}^T\boldsymbol{C}^{-1}}_{\boldsymbol{F}}\boldsymbol{\rho}\underbrace{\boldsymbol{H}^T\boldsymbol{C}^{-1}\boldsymbol{H}}_{\boldsymbol{G}}\boldsymbol{e}_\xi\right) = \frac{\delta}{\delta \boldsymbol{e}_\xi}\begin{bmatrix} z_1 \\ z_2 \\ z_3 \end{bmatrix} \tag{A.6}$$

$$z_m = \left(\sum_{i=1}^{3} \sum_{j=1}^{3} \underbrace{e_i F_{ij} \rho_j}_{\alpha_{ij}} \right) \cdot \left(\sum_{k=1}^{3} \underbrace{G_{mk} e_k}_{\beta_k} \right) \tag{A.7}$$

$$= \left(\sum_{i=l} \sum_{j=1}^{3} \alpha_{ij} \right) \cdot \left(\sum_{k=l} \beta_k \right) \tag{A.8}$$

$$+ \left(\sum_{i=l} \sum_{j=1}^{3} \alpha_{ij} \right) \cdot \left(\sum_{k=1, k \neq l}^{3} \beta_k \right) \tag{A.9}$$

$$+ \left(\sum_{i=1, i \neq l}^{3} \sum_{j=1}^{3} \alpha_{ij} \right) \cdot \left(\sum_{k=l} \beta_k \right) \tag{A.10}$$

$$+ \left(\sum_{i=1, i \neq l}^{3} \sum_{j=1}^{3} \alpha_{ij} \right) \cdot \left(\sum_{k=1, k \neq l}^{3} \beta_k \right) \tag{A.11}$$

$$i = k = l: \qquad z_m^{(1)} = \left(e_l \cdot \sum_{j=1}^{3} F_{lj}\rho_j \right) \cdot (G_{ml} e_l) \tag{A.12}$$

$$= e_l^2 \cdot \left(\sum_{j=1}^{3} F_{lj}\rho_j \right) \cdot (G_{ml}) \tag{A.13}$$

$$\frac{\delta z_m^{(1)}}{\delta e_l} = 2e_l \cdot \left(\sum_{j=1}^{3} F_{lj}\rho_j \right) \cdot (G_{ml}) \tag{A.14}$$

$$i = l, k \neq l: \qquad z_m^{(2)} = \left(e_l \cdot \sum_{j=1}^{3} F_{lj}\rho_j \right) \cdot \left(\sum_{k \neq l} G_{mk} e_k \right) \tag{A.15}$$

$$\frac{\delta z_m^{(2)}}{\delta e_l} = \left(\sum_{j=1}^{3} F_{lj}\rho_j \right) \cdot \left(\sum_{k \neq l} G_{mk} e_k \right) \tag{A.16}$$

$$i \neq l, k = l: \qquad z_m^{(3)} = \left(\sum_{i \neq l} e_i \cdot \sum_{j=1}^{3} F_{ij}\rho_j \right) \cdot (G_{ml} e_l) \tag{A.17}$$

$$\frac{\delta z_m^{(3)}}{\delta e_l} = \left(\sum_{i \neq l} e_i \sum_{j=1}^{3} F_{ij}\rho_j \right) \cdot (G_{ml} e_l) \tag{A.18}$$

$$i \neq l, k \neq l: \qquad z_m^{(4)} = \left(\sum_{i \neq l} \sum_{j=1}^{3} e_i F_{ij}\rho_j \right) \cdot \left(\sum_{k \neq l} G_{mk} e_k \right) \tag{A.19}$$

$$\frac{\delta z_m^{(4)}}{\delta e_l} = 0 \tag{A.20}$$

$$\frac{\delta}{\delta \boldsymbol{e}_\xi} \left(\boldsymbol{e}_\xi^T \boldsymbol{H}^T \boldsymbol{C}^{-1} \boldsymbol{\rho} \boldsymbol{H}^T \boldsymbol{C}^{-1} \boldsymbol{H} \boldsymbol{e}_\xi \right) = \tag{A.21}$$

$$= \begin{bmatrix} \frac{\delta z_1^{(1)}}{\delta e_1} + \frac{\delta z_1^{(2)}}{\delta e_1} + \frac{\delta z_1^{(3)}}{\delta e_1} + \frac{\delta z_1^{(4)}}{\delta e_1} & \cdots & \frac{\delta z_1^{(1)}}{\delta e_3} + \frac{\delta z_1^{(2)}}{\delta e_3} + \frac{\delta z_1^{(3)}}{\delta e_3} + \frac{\delta z_1^{(4)}}{\delta e_3} \\ \vdots & \ddots & \vdots \\ \frac{\delta z_3^{(1)}}{\delta e_1} + \frac{\delta z_3^{(2)}}{\delta e_1} + \frac{\delta z_3^{(3)}}{\delta e_1} + \frac{\delta z_3^{(4)}}{\delta e_1} & \cdots & \frac{\delta z_3^{(1)}}{\delta e_3} + \frac{\delta z_3^{(2)}}{\delta e_3} + \frac{\delta z_3^{(3)}}{\delta e_3} + \frac{\delta z_3^{(4)}}{\delta e_3} \end{bmatrix}$$

③ $$\frac{\delta}{\delta \boldsymbol{e}_\xi} \left(-\boldsymbol{H}^T \boldsymbol{C}^{-1} \boldsymbol{\rho} \right) = 0 \tag{A.22}$$

④ $$\frac{\delta}{\delta \boldsymbol{e}_\xi} \left(-\boldsymbol{e}_\xi^T \underbrace{\boldsymbol{H}^T \boldsymbol{C}^{-1} \boldsymbol{H}}_{\boldsymbol{M}} \boldsymbol{e}_\xi \underbrace{\boldsymbol{H}^T \boldsymbol{C}^{-1}}_{\boldsymbol{N}} \boldsymbol{\rho} \right) = \frac{\delta}{\delta \boldsymbol{e}_\xi} \begin{bmatrix} h_1 \\ h_2 \\ h_3 \end{bmatrix} \tag{A.23}$$

$$h_m = \left(\sum_{i=1}^{3} \sum_{j=1}^{3} e_i M_{ij} e_j \right) \cdot \left(\sum_{k=1}^{3} N_{mk} \rho_k \right) \tag{A.24}$$

$$i = j = l: \qquad h_m^{(1)} = e_l^2 M_{ll} \cdot \sum_{k=1}^{3} N_{mk} \rho_k \tag{A.25}$$

$$\frac{\delta h_m^{(1)}}{\delta e_l} = 2 e_l M_{ll} \cdot \sum_{k=1}^{3} N_{mk} \rho_k \tag{A.26}$$

$$i = l, j \neq l: \qquad h_m^{(2)} = \left(e_l \sum_{j \neq l} M_{lj} e_j \right) \cdot \left(\sum_{k=1}^{3} N_{mk} \rho_k \right) \tag{A.27}$$

$$\frac{\delta h_m^{(2)}}{\delta e_l} = \left(\sum_{j \neq l} M_{lj} e_j \right) \cdot \left(\sum_{k=1}^{3} N_{mk} \rho_k \right) \tag{A.28}$$

$$i \neq l, j = l: \qquad h_m^{(3)} = \left(\sum_{i \neq l} e_i M_{il} e_l \right) \cdot \left(\sum_{k=1}^{3} N_{mk} \rho_k \right) \tag{A.29}$$

$$\frac{\delta h_m^{(3)}}{\delta e_l} = \left(\sum_{i \neq l} e_i M_{il} \right) \cdot \left(\sum_{k=1}^{3} N_{mk} \rho_k \right) \tag{A.30}$$

$$i \neq l, j \neq l: \qquad h_m^{(4)} = \left(\sum_{i \neq l} \sum_{j \neq l} e_i M_{ij} e_j \right) \cdot \left(\sum_{k=1}^{3} N_{mk} \rho_k \right) \tag{A.31}$$

$$\frac{\delta h_m^{(4)}}{\delta e_l} = 0 \tag{A.32}$$

$$\frac{\delta}{\delta \boldsymbol{e}_\xi} \left(-\boldsymbol{e}_\xi^T \boldsymbol{H}^T \boldsymbol{C}^{-1} \boldsymbol{H} \boldsymbol{e}_\xi \boldsymbol{H}^T \boldsymbol{C}^{-1} \boldsymbol{\rho} \right) = \tag{A.33}$$

$$= \begin{bmatrix} \frac{\delta h_1^{(1)}}{\delta e_1} + \frac{\delta h_1^{(2)}}{\delta e_1} + \frac{\delta h_1^{(3)}}{\delta e_1} + \frac{\delta h_1^{(4)}}{\delta e_1} & \cdots & \frac{\delta h_1^{(1)}}{\delta e_3} + \frac{\delta h_1^{(2)}}{\delta e_3} + \frac{\delta h_1^{(3)}}{\delta e_3} + \frac{\delta h_1^{(4)}}{\delta e_3} \\ \vdots & \ddots & \vdots \\ \frac{\delta h_3^{(1)}}{\delta e_1} + \frac{\delta h_3^{(2)}}{\delta e_1} + \frac{\delta h_3^{(3)}}{\delta e_1} + \frac{\delta h_3^{(4)}}{\delta e_1} & \cdots & \frac{\delta h_3^{(1)}}{\delta e_3} + \frac{\delta h_3^{(2)}}{\delta e_3} + \frac{\delta h_3^{(3)}}{\delta e_3} + \frac{\delta h_3^{(4)}}{\delta e_3} \end{bmatrix}$$

We can now apply the well known method of steepest descent:

$$\text{in general}: \qquad \boldsymbol{x}_{n+1} = \boldsymbol{x}_n - \boldsymbol{A}^{-1} \boldsymbol{y}_n \tag{A.34}$$

$$\text{here}: \qquad \boldsymbol{e}_{\boldsymbol{\xi_{n+1}}} = \boldsymbol{e}_{\xi_n} - \boldsymbol{A}^{-1} \left(\boldsymbol{e}_{\xi_n} \right) \cdot \boldsymbol{f} \left(\boldsymbol{e}_{\xi_n} \right) \tag{A.35}$$

Bibliography

[1] P. Henkel, Reliable Carrier Phase Positioning, *PhD thesis*, Technische Universität München, **2010**

[2] C. Günther, Satellite Navigation, to appear, **2011**

[3] P. Henkel and P. Jurkowski, Verfahren und Vorrichtung zur Bestimmung der Relativpositionen zwischen zwei Empfängern und Verwendung der Vorrichtun zur Stabilisierung schwebender Lasten, *German Patent*, Appl. Num.: 10 2010 038 257.4, **Sep 2010**

[4] P. Jurkowski, P. Henkel, G. X. Gao and C. Günther, Integer ambiguity resolution with tight and soft baseline constraints for freight stabilization at helicopters and cranes, *accepted for ION ITM*, San Diego, USA, **2011**

[5] P. Henkel and C. Günther, Reliable Integer Ambiguity Resolution with Multi-Frequency Code Carrier Linear Combinations, *Proc. of ION GNSS*, pp. 1–11, Portland, USA, **2010**

[6] P. Henkel, Bootstrapping with Multi-Frequency Mixed Code Carrier Linear Combination and Partial Integer Decorrelation in the Presence of Biases, *Proc. of Int. Assoc. of Geod. Scient. Ass.*, Buenos Aires, Argentina, **2009**

[7] P. Henkel, V. Gomez and C. Günther, Modified LAMBDA for absolute carrier phase positioning in the presence of biases, *Proc. of Int. Techn. Meet. (ITM)*, pp. 642–651, Anaheim, USA, **2009**

[8] P. Henkel and C. Günther, Reliable Integer Ambiguity Resolution with Multi-frequency Mixed Code Carrier Combinations, *ION GNSS 2010: Session B1*, **2010**

[9] P. Henkel and C. Günther, Joint L/C Band Code and Carrier Phase Linear Combinations for Galileo, *International Journal of Navigation and Observation*, **2008**

[10] P. Buist, The Baseline Constrained LAMBDA Method for Single Epoch, Single Frequency Attitude Determination Applications, *Proc. of ION GPS*, pp. 2962–2973, Fort Worth, TX, USA, **2007**

[11] P. Teunissen, GNSS Ambiguity Bootstrapping: Theory and Application, *Proc. of KIS2001*, pp. 246–254, **2001**

[12] G. Giorgi, P. Teunissen and S. Verhagen, Reducing the Time-To-Fix for Stand-Alone Single-Frequency GNSS Attitude Determination, *Proc. of ION ITM*, pp. 526–534, San Diego, USA, **2010**

[13] G. Blewitt, Carrier-phase ambiguity resolution for the Global Positioning System applied to geodetic baselines up to 2000 km, *J. Geophys. Res.*, vol. 94, pp. 10187–10203, **1989**

[14] R. Dach, U. Hugentobler, P. Fridez and M. Meindl, Bernese GPS Software, version 5.0, **2007**

[15] P. de Jonge and C. Tiberius, The LAMBDA method for integer ambiguity estimation: implementation aspects, *Publ. of the Delft Geod. Comp. Centre, LGR-Series*, no. 12, pp. 1–59, **1996**

[16] R. Moenikes, O. Meister, J. Wendel and G. F. Trommer, Yaw Angle Estimation of VTOL-UAVs with the Extended LAMBDA Method and Low Cost Receivers, *Proceedings of the 2007 National Technical Meeting of The Institute of Navigation*, pp. 179–186, San Diego, CA, USA, **2007**

[17] P. Teunissen, The Lambda Method for the GNSS Compass, *Art. Satellites*, vol. 41, nr. 3, pp. 89–103, **2006**

[18] P. Teunissen, Adjustment theory – an introduction, *Series on Math. Geod. and Pos.*, TU Delft, The Netherlands, **2003**

[19] P. Teunissen, The least-squares ambiguity decorrelation adjustment: a method for fast GPS integer ambiguity estimation, *J. of Geodesy*, vol. 70, pp. 65–82, **1995**

[20] P. Teunissen, Least-Squares Estimation of the Integer GPS Ambiguities, Invited lecture, Section IV "Theory and Methodology", *Proc. of Gen. Meet. of the Int. Assoc. of Geodesy*, Beijing, China, pp. 1–16, **1993**

[21] P. Teunissen, G. Giorgi, P. Buist, Testing of a new single-frequency GNSS carrier phase attitude determination method: land, ship and aircraft experiments, *GPS Solutions*, **2010**